DEVELOPMENT OF LOW COST ELECTROSTATIC SPRAY-CHARGING SYSTEM FOR LIQUID FORMULATIONS

By

DIPAK S. KHATAWKAR

THESIS

Submitted in partial fulfilment of the requirement for the degree

Master of Technology
in
Agricultural Engineering

Faculty of Agricultural Engineering and Technology
Kerala Agricultural University

Department of Farm Power, Machinery and Energy
KELAPPAJI COLLEGE OF AGRICULTURAL ENGINEERING AND TECHNOLOGY,
TAVANUR – 679 573, MALAPPURAM DISTRICT,
KERALA
2016

DECLARATION

I hereby declare that this thesis entitled **'Development of Low Cost Electrostatic Spray-Charging System for Liquid Formulations'** is a bonafide record of research work done by me during the course of research and that the thesis has not previously formed the basis for the award to me of any degree, diploma, fellowship or associateship or other similar title of any other University or Society.

DIPAK S. KHATAWKAR

Tavanur
16/08/2016

CERTIFICATE

Certified that this thesis entitled **'Development of Low Cost Electrostatic Spray-Charging System for Liquid Formulations'** is a record of research work done independently by **Sri. Dipak S. Khatawkar** under my guidance and supervision and that it has not previously formed the basis for the award of any degree, diploma, fellowship or associateship to him.

Dr. Dhalin D.
(Chairman, Advisory Committee)
Assistant Professor,
(Farm Power, Machinery and Energy)
College of Agriculture – Vellayani,
Thiruvananthapuram.

Tavanur
16/08/2016

CERTIFICATE

We undersigned, members of the advisory committee of **Sri. Dipak S. Khatawkar**, a candidate for the degree of Master of Technology in Agricultural Engineering, majoring in Farm Power Machinery and Energy, agree that the thesis entitled **'Development of Low Cost Electrostatic Spray-Charging System for Liquid Formulations'** may be submitted by Sri. Dipak S. Khatawkar, in partial fulfilment of the requirement for the degree.

Dr. Dhalin D.
(Chairman, Advisory Committee)
Assistant Professor,
(Farm Power, Machinery and Energy)
College of Agriculture – Vellayani,
Thiruvananthapuram.

Dr. M. S. Hajilal
Professor and Dean,
Kelappaji College of Agricultural Engineering and Technology, Tavanur.

Dr. Jayan P. R.
Professor and Head,
Dept. of FPME, Kelappaji College of Agricultural Engineering and Technology, Tavanur.

Dr. Shaji James P.
Professor,
(Farm Power, Machinery and Energy)
Kelappaji College of Agricultural Engineering and Technology, Tavanur.

Er. Shivaji K. P.
Assistant Professor,
(Farm Power, Machinery and Energy)
Kelappaji College of Agricultural Engineering and Technology, Tavanur.

Date : 16.08.2016
Place : Tavanur

External Examiner

ACKNOWLEDGEMENT

With due respect, I record my gratitude and utmost indebtedness to ***Dr. Dhalin D.****, Assistant Professor, College of Agriculture – Vellayani and Chairman of the Advisory Committee for his avuncular advice, guidance, encouragement and creative criticism during the course of this research work and in the preparation of the thesis.*

It is my greatest pleasure to acknowledge the sincere guidance and valuable help rendered to me by ***Dr. M. S. Hajilal****, Dean, Kelappaji College of Agricultural Engineering and Technology, Tavanur.*

It is my privilege to express heartfelt thanks to ***Dr. Jayan P. R.****, Professor and Head, Department of Farm Power, Machinery and Energy, Kelappaji College of Agricultural Engineering and Technology, Tavanur for his excellent advice and help during each step of this research work as well as ingenious criticism during preparation of the thesis.*

I express my immense gratitude towards ***Dr. Shaji James P.****, Professor, Department of Farm Power, Machinery and Energy, Kelappaji College of Agricultural Engineering and Technology, Tavanur and member of Advisory Committee for his valuable critics and help during preparation of the thesis.*

It is my pleasure to express heartfelt reverence to ***Er. Shivaji K. P.*** *Assistant Professor, Department of Farm Power, Machinery and Energy, Kelappaji College of Agricultural Engineering and Technology, Tavanur and member of Advisory Committee for his guidance during this research work.*

I gratefully acknowledge the support and encouragement extended by ***Dr. Rajesh G. K.****, Associate Professor and Academic Officer, Food and Agricultural Process Engineering, Kelappaji College of Agricultural Engineering and Technology, Tavanur.*

I wish to place on record my thanks to library staff for providing access to library that was crucial in successful completion of this project work.

*Words may prove trivial if I attempt to depict my gratitude **Dr. Xavier J.**, Professor and Head, Department of Agricultural Engineering, College of Agriculture – Vellayani for his help during the research work.*

The award of Junior Research Fellowship by Kerala Agricultural University is also greatly acknowledged.

I also extend my sincere thanks to my near and dear ones for their warm blessings and unfailing support which enabled me to have everything at reach.

*Above all, I bow my head to **The God Almighty**, whose blessings filled me with power to complete this work.*

*At last but not the least, I am short of words to express my gratitude towards my **Beloved Parents and all family members** for their endless love, blessings, inspiration and great support.*

Dipak S. Khatawkar

TABLE OF CONTENTS

Chapter	Title	Page No.
	LIST OF TABLES	i
	LIST OF FIGURES	ii
	LIST OF PLATES	v
	SYMBOLS AND ABBREVATIONS	vi
I	INTRODUCTION	1
II	REVIEW OF LITERATURE	3
III	MATERIALS AND METHODS	24
IV	RESULTS AND DISCUSSION	51
V	SUMMARY AND CONCLUSION	74
	REFERENCES	
	APPENDICES	
	ABSTRACT	

LIST OF TABLES

Table No.	Title	Page
1	Effect of electrode potential on CMR	67
2	Deposition efficiency	69
3	CMR comparison between commercial and developed system	70
4	Cost Economics of developed system	73

LIST OF FIGURES

Fig. No.	Title	Page
1	Polarity of water molecule	7
2	Electrostatic charge on plants	7
3	Electrostatic induction spray charging system	26
4	Diode-Pump Rectifier	28
5	Cockcroft-Walton voltage multiplier	28
6	High Voltage generator	30
7a	Model I : Exposed electrode placement assembly	31
7b	Model I : Exposed electrode placement assembly (Isometric view)	31
8	HV-Charging electrode	33
9	Nozzle Assembly of the knapsack mist blower	33
10	Schematics of Faraday' Cage	38
11	Model II : Redesigned nozzle with reduced spray-jet outlets	40
12	Self-Atomizing hydraulic nozzle (Isometric View)	40
13a	Self-Atomizing hydraulic nozzle (Sectional View)	41
13b	Adapter for nozzle fitment (Sectional View)	41
14a	Model IV : Embedded electrode assembly – Sectional view	43
14b	Model IV : Embedded electrode assembly – Isometric view	43
15a	Model V : Narrow embedded electrode assembly (Sectional view)	44
15b	Model V : Narrow embedded electrode assembly (Isometric view)	44
16	Effect of electrode voltage potential on charge induction (CMR) at 50 cm head of nozzle and EPP - 0 mm	57

17	Effect of electrode voltage potential on charge induction (CMR) at 50 cm head of nozzle and EPP - 5 mm	57
18	Effect of electrode voltage potential on charge induction (CMR) at 50 cm head of nozzle and EPP - 10 mm	58
19	Effect of electrode voltage potential on charge induction (CMR) at 50 cm head of nozzle and EPP - 15 mm	58
20	Effect of electrode voltage potential on charge induction (CMR) at 100 cm head of nozzle and EPP - 0 mm	59
21	Effect of electrode voltage potential on charge induction (CMR) at 100 cm head of nozzle and EPP - 5 mm	59
22	Effect of electrode voltage potential on charge induction (CMR) at 100 cm head of nozzle and EPP - 10 mm	60
23	Effect of electrode voltage potential on charge induction (CMR) at 100 cm head of nozzle and EPP - 15 mm	60
24	Effect of electrode voltage potential on charge induction (CMR) at 150 cm head of nozzle and EPP - 0 mm	61
25	Effect of electrode voltage potential on charge induction (CMR) at 150 cm head of nozzle and EPP - 5 mm	61
26	Effect of electrode voltage potential on charge induction (CMR) at 150 cm head of nozzle and EPP - 10 mm	62
27	Effect of electrode voltage potential on charge induction (CMR) at 150 cm head of nozzle and EPP - 15 mm	62
28	Effect of electrode voltage potential on charge induction (CMR) at 200 cm head of nozzle and EPP - 0 mm	63
29	Effect of electrode voltage potential on charge induction (CMR) at 200 cm head of nozzle and EPP - 5 mm	63
30	Effect of electrode voltage potential on charge induction (CMR) at 200 cm head of nozzle and EPP - 10 mm	64
31	Effect of electrode voltage potential on charge induction (CMR) at 200 cm head of nozzle and EPP - 15 mm	64
32	Effect of electrode voltage potential on charge induction (CMR) at 250 cm head of nozzle and EPP - 0 mm	65

33	Effect of electrode voltage potential on charge induction (CMR) at 250 cm head of nozzle and EPP - 5 mm	65
34	Effect of electrode voltage potential on charge induction (CMR) at 250 cm head of nozzle and EPP - 10 mm	66
35	Effect of electrode voltage potential on charge induction (CMR) at 250 cm head of nozzle and EPP - 15 mm	66
36	Effect of Charge carrying distance on CMR	72
37	Charge carrying capacity: Developed system (Model V) with five charging voltages Vs. Commercial ESS MBP90 sprayer	72

LIST OF PLATES

Plate No.	Title	Page
1	Powered knapsack mist blower	26
2	High Voltage generator with pulse generator	30
3	High Voltage Measuring System	36
4	RS-232 Computer Interface-Data Logging Software	36
5	Faraday' Cage for spray cloud charge measurement	38
6	Electrostatic induction charging unit attached to the powered knapsack mist blower	46
7	Experimental Setup	46
8	Spray impinged Bromide paper	48
9	Window of Image-J-2016 software during droplet spectrum analysis	48
10	Spray Deposition on upper leaf surface - Electrostatic Sprayer	71
11	Spray Deposition on under leaf surface - Electrostatic Sprayer	71
12	Spray Deposition on Pepper leaf surface – Uncharged Air-assisted Spray	71

LIST OF SYMBOLS AND ABBREVIATIONS

^{o}C	Degree Celsius
%	Percentage
±	plus or minus
µA	micro ampere
µC	micro coulomb
µF	micro farads
µm	micro meter
µV	micro volt
$\mu C.kg^{-1}$	micro coulomb per kilogram
AC	Alternating Current
ANOVA	Analysis of variance
AP	Action Potential
CCD	Charge Coupled Device Camera
cm	centimeter
cm^3	cubic centimeter
CMR	Charge to Mass Ratio
CRD	Completely Randomized Design
C-W	Cockroft-Walton

DC	Direct Current
dia.	Diameter
DMM	Digital Multimeter
EHD	Electro-Hydro dynamics
EIC	Electrostatic Induction Charging
EPP	Electrode placement position
ESS	Electrostatic Spraying Systems
GLM	General Linear Model
HV	High Voltage
HVDC	High Voltage Direct Current
HP	Horse Power
IC	Integrated Circuit
kPa	kilo-Pascal
kV	kilo-volt
LAI	Leaf Area Index
LD-HP	Low Discharge High Pressure
lpm	Litre per minute
LSD	Least Significant Difference
m^3	cubic meter

MΩ	Mega-ohm
mA	milli ampere
mm	millimeter
NMD	Number median diameter
No.	Number
OD	Outer diameter
ppm	parts per million
PTO	Power take-off
SS	Stainless steel
VMD	Volume mean diameter
VP	Variation Potential
WSP	Water Sensitive Paper

CHAPTER I
INTRODUCTION

In commercial agriculture, plant protection chemicals are vital for profitability, low food prices and for maintaining adequate food supply. Without them, crop losses could be as high as 50 per cent for field crops and up to 100 per cent for fruit crops and greenhouse ornamentals. The demand for plant protection machinery in India is increasing every year. In the country, the powered knapsack mist blower is one of the most popular and versatile pesticide application equipment because of its simplicity, ease of operation and inexpensiveness. But still these sprayers have to overcome the problems of low target deposition, distribution and penetration into the plant canopies.

The introduction of electrically charged sprays for agricultural application can provide greater control of droplet transport with impending reduction of wastage. The use of electrostatic spraying can increase the application efficiency by about 80 per cent with 60 per cent less spray chemical ingredients (Lane and Law, 1982). Electrostatics, the study of static electricity, the surface phenomenon governing electric charges accumulated on a body as explained by Coulomb's law. It has significant potential on application of agricultural liquid formulations since charged particles can perform uniform spray coverage with considerably less quantity.

The three methods which can be adopted to charge the fluid spray are conduction charging, corona charging and induction charging. Conduction charging involves direct application of high voltage potential to the spray fluid by conduction. But this method requires higher power supply and has the hazard of getting high voltage shock to the operator. Corona charging uses the corona discharge field to charge the spray particles passing through it, which also has drawbacks of life hazard and may cause chemical changes to the subjected spray material. The method of ‘Electrostatic Induction Charging’ (EIC) works on the non-contact charge induction on the subjected spray fluid passing through the high voltage electrical field. As the method has no direct contact with the working

fluid, the chances of getting high voltage shock to the operator are negligible and the power consumption is also considerably lower than the other methods. This made the electrostatic induction charging as the best suitable method for charging agricultural spray liquids. Hence the method was adopted for this study due to its known advantages over other charging methods like high charge transferability, less hazardous to life and simplicity in construction.

Majority of agricultural chemicals are applied as water based formulations. Water has a polar molecular structure and has a large value of electric dipole moment due to hydrogen covalent bonds. The electron-pair forming covalent bond gets attracted towards the oxygen atom and as a result oxygen side gets slight negative polarity and hydrogen side gets slight positive polarity which induces an electric dipole moment within the water molecule. On the basis of electro-chemistry of polar molecules, fine water droplets can be charged electrostatically. The plants grounded to the earth shall be at zero potential, even though the metabolic processes of living plant body induces slight positive charge on the plant. But this charge has been found to be distributed asymmetrically on plant surface, concentrated near the sharp protruding body parts such as leaf tips, spikes and especially floral parts.

In India, only a few attempts have been made so far in developing and testing indigenous electrostatic spray charging systems. Moreover, the development of an economical electrostatic spray charging system for an existing sprayer will be a boon to the Indian farmer. Hence, the development of an electrostatic induction charging attachment to a conventional “duro mist” nozzle was contemplated with the following specific objectives:

1. To develop a low cost electrostatic nozzle and charging system compatible to a DC power source.
2. To study the dynamic charge acquisition and spray chargeability of the developed system.
3. To evaluate the depositional characteristics of the charged spray on plant targets.

CHAPTER II

REVIEW OF LITERARUTRE

In this chapter, a brief review of research works carried out in the development of an effective electrostatic agricultural spray charging system and the methods adopted for its evaluation are presented.

2.1 Static Electricity

Electrostatics deals with the study of static electricity, the surface phenomenon governing electric charges accumulated on a body as explained by Coulomb's law. It has significant potential on application of agricultural chemicals for improving the uniform spray coverage with considerably less quantity.

Coulomb's law is an experimental law formulated in 1785 by the French colonel, Charles Augustin de Coulomb, which states that the force (*F*) between two point charges Q_1 and Q_2 acts along the line joining them and directly proportional to the product of charges and inversely proportional to the square of distance (*R*) between them. It can be expressed mathematically as,

$$F \propto \frac{Q_1.Q_2}{R^2} \qquad \text{and} \qquad F = \frac{K.Q_1.Q_2}{R^2}$$

Where, *K* is the proportionality constant. In SI units, charges Q_1 and $Q_2$are in coulombs (C), the distance *R* is in metre (m), the force *F* is in newton (N) and $K=1/4\pi\varepsilon_0$. The constant $\varepsilon_0$is known as the *permittivity of free space* (in farads per meter) and has the value,

$$\varepsilon_0 = 8.854 \times 10^{-12} \quad F\,m^{-1} \quad = \frac{10^{-9}}{36\pi} \quad F\,m^{-1}$$

Therefore,

$$K = \frac{1}{4\pi\varepsilon_0} = 9 \times 10^9 \;\; m\,F^{-1}\; or\; N.m^2C^{-2}$$

2.1.1 Static electricity present in the plants and Electrostatic spraying

Lane and Law (1982) conducted study on transient charge transfer in living plants undergoing electrostatic spraying. An electric field generator was used to create time varying electric field in the vicinity of grounded cotton plant. The high voltage (HV) electrode was constructed from 1.04 m x 1.04 m sheet of galvanized steel with its edges covered by copper tube to reduce unwanted corona discharge and placed in horizontal distance of 1.45 m from the ground with Teflon insulation. An electrometer with operational mode was used for measurement of charge transfer through the plant. The output of electrometer was fed into storage oscilloscope to record the time varying charge flow through the plants. The electrode potential was held constant at -15 kV for the entire experiment. The drought stressed cotton plants showed reduction in charge transfer compared to plants in normal conditions, in the range of 3.0 to 4.0 with respect to time.

Jorg and Launter (2006) studied about electrical signals in plants, the measurement techniques and their physiological significance. They conducted experiments on *Mimosa pudica* and *Dionea muscipula* with artificial generation of electrical signals to resemble the environmental stimuli, such as light, temperature, touch or wounding etc. which generated Action Potential (AP) and Variation Potential (VP) within the plant organ. In which APs were fast and propagated very rapidly at speed of 10 – 20 $mm.s^{-1}$, whereas VPs are relatively slower wave potentials. These may be generated due to wounding, organ excision or flaming and was studied in cucumber and pea seedlings. Physiological effects in *Dionea* revealed that, catching starts with release of Calcium-ion into cytosol by mechanical pressure of one of trigger hairs and subsequently APs generated without any response of trap. If any trigger hair get bent no later than 40 s after the first, a second fast AP evoked to close the trap.

Mouel *et al.* (2010) studied electric potential variations in a standing tree and electricity present in the atmosphere. The investigations were done on the trunk of the standing poplar tree equipped with electrodes along its height of 0.5 m to 10.5 m. The results were noticed by Keithley Electrometer for amplitude and

duration which gradually increased with the heights 0.5 m to 10.5 m from ground at increments of 50 cm between two consecutive stainless steel electrodes (6 mm dia.). Electrodes were hammered gently into the trunk up to a depth of 15mm with sampling interval in measurements of one minute using Keithley 2701 electrometer with input impedance larger than 100 MΩ. They observed that there was no difference between the plots of positive and negative signals, plotted against the height respectively. In few cases the plot was straight with a slope of 0.1 to 5.0 $mV.m^{-1}$.

Oyarace and Luis (2010) investigated electrical signals in Avocado trees against light and water availability. Electrical potentials generated within Avocado trees were monitored continuously using non-polarizable Ag/AgCl micro-electrodes inserted at different positions along the trunk. These electrodes include silver wire of 0.35 mm dia. in stainless steel needle of 0.5 mm dia. Electrodes were connected to 20-channel multi-voltmeter digital data logger (Keithley 2701) with compatible switching board (Keithley 7700). The measurements were taken during dawn, morning, afternoon and at night with irrigated and non-irrigated conditions. It was observed that negative polarity voltage potential developed in the range of 77.85 to 109.68 mV during dawn, 74.37 to 109.16 mV during morning, 68.13 to 106.91 mV during afternoon and 72.70 to 108.25 mV during night.

2.2 Electrostatic Particle Charging Methods

There are three methods to charge the fluid spray, viz. conduction charging, corona charging and induction charging. Conduction charging which involves direct application of high voltage potential to the spray fluid by conduction. However, this method requires higher power supply and has hazard of getting high voltage shock to the operator.

Corona charging uses the corona discharge field to charge the spray particles passing through it, which also has drawbacks of life hazard and may cause chemical changes to the subjected spray material. The method of Electrostatic induction charging (EIC) works on the non-contact charge induction

on the subjected spray fluid passing through the high voltage electrical field. As the method has no direct contact with the working fluid, the chances of getting high voltage shock to the operator are negligible and the power consumption is also considerably lower than the other methods. This makes the Electrostatic Induction charging as the best suitable method for charging agricultural spray liquids to adopt in this study.

Water has a polar molecular structure and a large value of electric dipole moment due to hydrogen covalent bonds. The electron pair forming covalent bond gets attracted towards the oxygen atom and as a result oxygen side gets slight negative pole and hydrogen side slight positive pole which induces electric dipole moment within the water molecule (Fig. 1). On the basis of electro-chemistry of polar molecules, fine water droplets can be charged electrostatically and therefore possibly pollen grains also.

The plants grounded to the earth shall be at zero potential, though in nature due to the metabolic process of living plant body induces slight negative charge on the plant (Fig. 2). But this charge has been found to be distributed asymmetrically on plant surface, concentrated near the sharp protruding body parts such as leaf tips, spikes and especially floral parts.

2.2.1 Voltage Amplification Unit and Electrostatic Induction Spray Charging

Smith *et al.* (1977) conducted study on AC charging of agricultural sprays and its effectiveness. A controllable DC voltage supply unit and three different charging annuli were used with charging voltage stepped in 4.3, 8.2, 12.5 and 16.5 kV with frequency range of 1040 to 1975 Hz. The spray nozzle operated at three constant pressures viz. 173, 276 and 380 kPa and for charging 0.8, 11.5 and 15 kV potentials were used in a square wave form. The 15 kV square wave form AC charging produced more number of small droplets under 50, 20 and 10 µm, so that charge per droplet could be higher and droplet voltage was measured with Keithley 614B Electrometer which showed values in the range of 50 mV to 175 mV for charging voltage 5 kV to 15 kV.

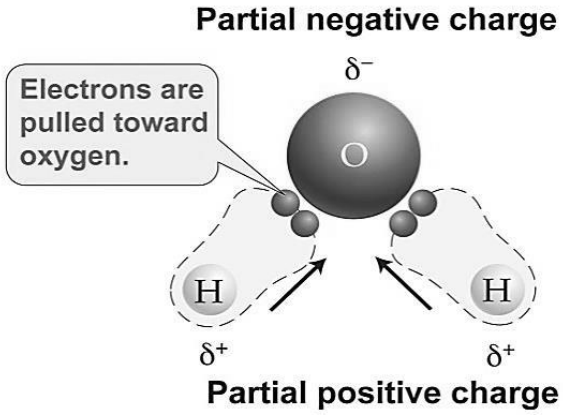

Fig. 1. Polarity of water molecule

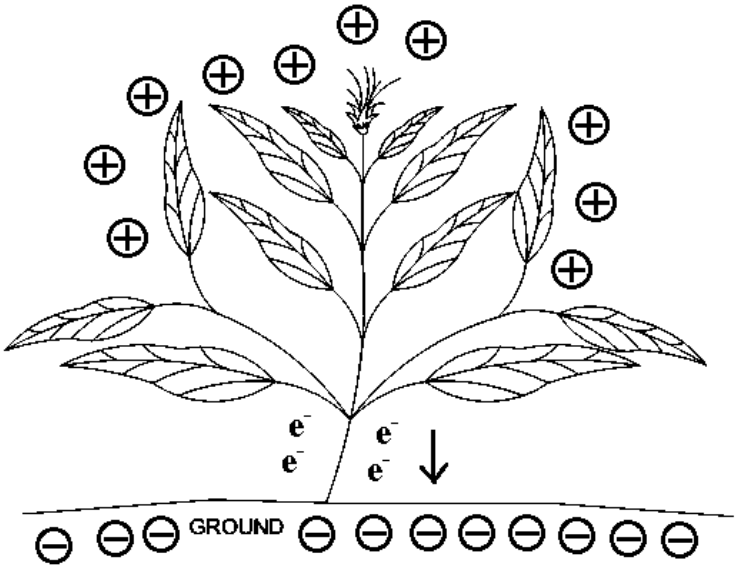

Fig. 2. Electrostatic charge on plants

Anantheswaran and Law (1979) developed an electrostatic spray charging nozzle for charging pesticide spray droplets by induction. The charging unit was operated by 12V DC battery, which gave an output voltage of -30 kV. For experimental analysis voltage given to the metal plate electrode varied from 0 to -30 kV, in steps of 10 kV. Also, a dielectric barrier type precipitator was evaluated, made of polythene sheet stretched over a square plexi-glass, which accumulated negative charges on its surface. Later these charges would repel spray droplets downward towards the turf grass. The deposition was found to be increased significantly on increasing inclination angle. In conjunction with dielectric barrier, deposition was observed to be increased by 3.6 folds compared to uncharged spray.

Carlton and Bouse (1980) designed, developed and evaluated an electrostatic spray charging spinning nozzle for aircraft. The rotational speed of the spinner and hence the droplet size was altered by regulating motor voltage. Spray charging efficiency increased with increase in spinner speed and CMR about 2 x 10^{-2} C.kg^{-1}. The experiments showed that electrostatically charged spray deposition may exceed that of uncharged spray counterpart by 800 per cent.

Gupta *et al.* (1994) designed and developed a knapsack type electrostatic spinning disc sprayer, of which charging system was consisted of 12 V DC wet cell rechargeable battery and HVDC power supply (Model-C30, Venus Scientific Inc., NY). Field applications were conducted with 1.2 kV charging potential, 50 ml.min^{-1} liquid flow rate and 2000 to 3000 rpm spinning disc speed. The results gave CMR from the charging system in the range of 1.0 to 1.2 mC.kg^{-1} with 169 μm mean droplet size. It was observed that, operator's contamination due to drifting chemical was reduced significantly due to rear mounted spray boom.

Luciana and Cramariuc (2009) conducted experiments on electro-hydrodynamic (EHD) spray injector including direct injector conduction charging, direct charging through open electrode and charging by induction with insulated electrode and grounded injector. DC high voltage ranging from 0 to 6 kV was used to charge the spray particles with liquid flow rate between 0.1 to 0.4 ml·s^{-1}

and two-stage Faraday cage and collector were used to measure the cloud current. They found induction charging as the most efficient method which shown optimum charge to mass ratio of 5 $\mu C \cdot g^{-1}$ at 3 kV with flow rate at 0.3 $ml \cdot s^{-1}$, with no electrical hazards and power loss.

Maynagh *et al.* (2009) evaluated electrostatic induction charging sprayer with ultrasonic (30 kHz) nozzle for different parameters such as electrode radius, voltage level, air velocity and electrode placement. The tests were performed with varying flow rate (5 to 25 $ml \cdot min^{-1}$), voltage levels (1.5 to 7 kV), airflow speeds, electrode radius (10 and 15 mm) and its horizontal position (1 to 10 mm) from nozzle tip. They found optimum CMR of 1.032 $\mu C \cdot g^{-1}$ at 7 kV voltage; 23 $m \cdot s^{-1}$ airflow speed, electrode radius and placement were 15 mm and 10 mm respectively, while liquid flow rate was kept at 5 $ml \cdot min^{-1}$ to reduce electrode wetting.

Almuhanna and Maghirang (2010) developed and evaluated a charge measuring device for measuring the net CMR induced on the filter with an electrometer. The device was tested using different kinds of airborne particles viz. corn starch, sodium bicarbonate, positively and negatively charged water spray and uncharged water spray. The device consisted of two conducting enclosures, one enclosed and insulated from another. It was electrically connected to the electrometer input (Keithley Instru. Inc., OH) and having particle filter with backup metal screen (Filter type – AE, SKC84-PA). Calibration circuit was made and used to generate known charges with variable DC voltage supply (B.K. Precision Triple, MaxTech Instru. Corp., Chicago) with 1, 2, 3 V DC fixed voltages and three different capacitors of 0.1µf, 0.01µf and 0.001µf. Electrostatic Spraying Systems (ESS, Watkinsville) sprayer was used to charge the water spray. The device had been showing reliable readings and good repeatability. With induction charging, significantly large CMR values (i.e. -6.5 mC kg^{-1} for negatively charged water spray and +7.2 mC kg^{-1} for positively charged water spray) were observed by the developed CMR measuring device, which were close

to CMR value (-6 mC kg^{-1}) specified by the manufacturer (ESS, Watkinsville, GA).

Yu *et al.* (2011) developed an axial flow air assisted ultra-low volume electrostatic sprayer with high voltage (20 kV) corona charging device. The sprayer was evaluated in laboratory as well as field for the parameters like CMR to corresponding voltage levels, droplet size, deposition uniformity and pest mortality against *micro-melalopha troglodyte fungi* on roadside forestry trees. Spraying was performed with charge as well as without charge on both sides of row along 10 km length. Performance of electrostatic spray was reported in terms of pest mortality, which was observed to be higher (95.40 %) over non-electrostatic spray (74.80 %), while CMR value observed to be 2.35 $mC \cdot kg^{-1}$ with 80.80 µm droplet size at 20 kV.

Mamidi *et al.* (2012) developed electrostatic hand pressure swirl nozzle knapsack sprayer for small crop growers and evaluated different parameters as electrode position, charge to mass ratio, spray deposition and effect of applied pressure on droplet size and breakup length. Twin hole swirl disc with 0.8 mm orifice and copper ring electrode connected to programmable 10W HVDC module (EMCO-F101) ranging from 0 to 10 kV was used. The placement of ring electrode was varied from 1 to 6 mm and manual hand pressure knapsack pump with output pressure from 0 to 2.82 $kg \cdot cm^{-2}$ was used to drive the swirl nozzle. Cloud current (A) and mass flow rate ($kg \cdot s^{-1}$) were measured at 2.11 $kg \cdot cm^{-2}$ pressure and 3.3 kV voltage which by which they found optimum CMR value and droplet size as 0.37 $mC \cdot kg^{-1}$ and 100 µm respectively, while electrode placed at 4.5 mm from orifice.

Robson *et al.* (2013) conducted a study on charge to mass ratio and liquid deposition efficiency of electrostatic spraying method. ESS-MBP 4.0 induction charging sprayer model was used for the experiment and Faraday cage equipped with digital multi-meter was used for chargeability analysis. The sprayings were done at distances 0, 1, 2, 3, 4 and 5 m from the Faraday cage and charge readings

were obtained from digital multimeter. Liquid discharge rate (lpm) was measured with graduated cylinder with precision of 5 ml. The highest charge-to-mass ratio was found to be 4.11 $mC \cdot kg^{-1}$ for the closest distance and it gradually decreased to 1.38, 0.64, 0.31, 0.017 and 0.005 $mC \cdot kg^{-1}$ for the corresponding distances 1, 2, 3, 4 and 5 m resp.

Patel *et al.* (2015) developed and analyzed an air assisted electrostatic spray charging nozzle for agricultural pesticide application in liquid form. Experiments were conducted to assess the parameters viz. charge to mass ratio (CMR), spray pattern, uniformity of deposition and coverage by using Water Sensitive Paper (WSP) method. Chargeability was tested with Faraday cage and digital multimeter under +20 kV High Voltage DC power supply. Plants were sprayed electrostatically as well as non-electrostatically under all other identical conditions with WSPs mounted on front and back side of leaves at random locations in canopy. After 20 minutes of spraying, WSP samples were collected and analyzed with IMAGE-J Scanner based system. Analysis showed that 2 to 3 times increase in leaf top deposition in electrostatic spray over non-electrostatic spraying, also observed that under leaf deposition has been enhanced by 4 to 5 times.

2.3 Measurement of Spray Charge Acquisition

Law (1975) conducted study on charge measurement of agricultural particles and developed an electrostatic induction instrument for tracking and charge measurement of airborne particles. Water held in variable-head glass reservoir was allowed to slowly drip from the blunt end of the hypothermic needle at the rate of 1 drop per 5 seconds. A negative charge was imparted on droplets by maintaining the needle at selected negative high voltage potential. A smooth induction electrode of 14 mm inner diameter and 3 mm thickness was positioned concentrically with and 6 mm below the tip of the needle. Keithley 600B electrometer was used for charge measurements and connected vertical deflection oscilloscope. A small Faraday's cage was positioned in a Teflon insulator at the

base of the apparatus. The average charge (- q) was determined experimentally by collecting and counting the number of drops acquired by Faraday's cage. Particle charge as high as - 4.25 x 10^{10} and - 2.45 x 10^{10} coulombs were attained and corresponded to CMR values as -2.5 x 10^{-5} C.kg^{-1} and -6 x 10^{10} C.kg^{-1} with – 2.5 kV needle potential.

Bode and Bowen (1991) conducted study on spray distribution and charge-mass ratio of electrostatically charged agricultural sprays. Spray droplet size was analyzed with Fleming Particle Size Analyzer at flow rates of 25, 50 and 75 ml.min^{-1} and spinner disc speed of 2000, 3000, 4000 and 5000 rpm for both charged and uncharged particles. For charged application a positive (0.5 to 3.0 kV) high voltage (HV) potential from HV power supply Model H-30 Ferrant Int., N.Y. was used. An Aluminium cup with 75 cm diameter and 50 cm height was used to intercept all the spray. Charged spray imparted an equal and opposite charge on the cup and was measured by Keithley 614 Electrometer. The measured droplet size was in the range of 115 to 203 µm without charging and 109 to 183 µm with charging. At all conditions studied, droplet size reduced by 1 to 10 per cent due to charging was observed. At peak level of charging from 0.5 kV to 3.0 kV, CMR was achieved in the range of 1.0 mC.kg^{-1} to 2.5 mC.kg^{-1} at spinner speed 3000 to 4000 rpm. The spray deposition efficiency was in the range of 55 to 94 per cent and relative increase due to charging was observed to be 1.6 to 2.0 fold over uncharged spray.

Kihm *et al.* (1991) conducted both laboratory as well as field experiments on bipolarly charged aircraft sprays in order to assess the deposition characteristics with DC motor driven serrated cup atomizers with induction charging ring electrode. Laboratory experiment was consisted of 40 hp motor driven blower at 175 km.h^{-1} air velocity, 55 mm diameter serrated cup atomizer with ring electrode having outer diameter of 63 mm and thickness of 1.6 mm. The clearance between Aluminium ring electrode and spinning cup edge was 2 mm axially and 2.4 mm radially. Malvern 2600D Aerosol sizer and charge collector Faraday's cage comprising of needle, plane mesh and concave mesh collector

were used for droplet size analysis and spray cloud charge measurement respectively. Whereas field apparatus was consisted of 60 m long movable stand with 40 WSPs and Cessna Model P206B agricultural aircraft with 10 atomizers cruising altitude 3 m at 175 $km.h^{-1}$ speed. CMR values were observed at 9000 and 12000 spinner rpm as 0.008 $C.kg^{-1}$ and 0.01 $C.kg^{-1}$ respectively. Field experiments showed increase of 45 percent in charged spray. However, the droplet size with bipolarly charged spray showed higher value than uncharged one.

Law and Scherm (1991) conducted an experiment on electrostatic application of plant disease bio-control agent against fungal infection on Blueberry. Electric characters of plant flower were determined in terms of resistance and resistivity. Application tests were carried for three setups as, hydraulic nozzle, electrostatic nozzle with charge-off and electrostatic nozzle with charge-on. Where, applied induction voltage for spray charging was set at 1.09 kV and corresponding CMR of -7.8 $mC.kg^{-1}$. Electrostatic charged spray application showed 4.5 time more deposition on target than other two methods and better viability for colony forming units.

Carlton *et al.* (1995) investigated an electrostatic charging of aerial spray to determine its depositional advantages. Three spray charging treatments were employed as, the use of dual power supply which provided bi-polar charge polarities of one wing-boom vs. the opposite one, low frequency alternating direct current which provided along the flight path alternating (+) and (-) sectors of unipolar charged spray and No-charging but maintaining all other parameters identical to first and second treatments. The spray deposition data was obtained by using the Leaf-wash method with fluorescence tracer. Statistical analysis indicated bi-polar charging to be superior over other two treatments, enhancing the spray deposits. The plant canopy penetration was achieved by horizontal drift forces. The research established that a level of Q/M = 2.64 $mC.kg^{-1}$ (CMR) was required to achieve expected improvement in spray deposition on targets.

2.4 Depositional Characteristics of electrostatically charged spray

Law and Michael (1981) conducted chargeability evaluation in laboratory with field sprayer simulator, which dispensed charged spray as it passed over stationary plants. The morphologies tested were mature cabbage, broccoli, mature cotton plants and corn plants. Three embedded-electrode spray charging nozzles were used for evaluation purpose with 73 $ml.min^{-1}$ flow rate per nozzle, which corresponded to 9.4 $lit.ha^{-1}$. The area density values of tracer particles deposited on foliar target was observed between 150 to 200 $ng.cm^{-2}$, with cloud current ranged 6 to 8 µA for electrostatic sprayer. Whereas, the depositional density was observed in the range of 50 to 75 $ng.cm^{-2}$ for conventional sprayer.

Lake and Merchant (1984) conducted wind tunnel experiments for the development of mathematical model for spray deposition in barley crop with an electrostatic sprayer. They reported that charging increased deposits on vertical target and tended to decrease deposits on upper surface of horizontal targets. Both the effects were significant with the smaller nozzles and independent of nozzle height.

Law and Cooper (1988) conducted study on mass transfer of fluorescent tracer onto front and back sides of the target deployed through a large scale grid. Mass transfer was determined for comparison between charged and uncharged spray from air-atomizing electrostatic nozzle and conventional hydraulic nozzle respectively. Depending on target location, electrostatically charged spray achieved higher deposition (1.5 to 2.4 fold over uncharged spray). The highest electro-deposition benefit was achieved on target back surfaces. Deposition of charged droplets did not surpass that achieved with 370 µm VMD droplets from conventional hydraulic orchard spraying nozzles.

Gupta *et al.* (1989) conducted experiments on a prototype of hand held electrostatic spray charging unit with spinning disc atomizer. Charging system consisted of Venus C-30 power supply unit having maximum output of 3 kV and 500 µA current with 5 to 12 V DC input. The spray liquid used was deionized water with 2 $g\ l^{-1}$ of fluorescent tracer (Fluorescent Sodium). The standard solvent

of 2% ethanol was used to wash-off the tracer from targets. Air gap of 1.8 mm was kept between spinning disc and Aluminium ring electrode. A two-fold increase in deposition was found with charged spray than compared to uncharged one.

Walker *et al.* (1989) conducted field evaluation of different pesticide spray atomizers for weed control in soybean cultivation. Research plots were consisted of 4 rows of soybean spaced at 102 cm and 18.3 m long under study period of 6 years. The spray atomizers taken into the study were rotary atomizer from Micron Corp., Sprayrite Mfg. Inc., Spraying Systems Co., Electrostatic prototype by FMC Corp., Air-atomizing nozzle by Spraying Systems Co. and Air-atomizing electrostatic prototype by Parker-Hamifin Corp. These different nozzles were compared with the conventional fan-type spray nozzle. They observed that non-conventional atomizers did not out-perform significantly as compared to conventional hydraulic sprayers based on broad leaf weed control over foliar applied chemicals.

Gupta *et al.* (1992) conducted field experiments to compare the deposition pattern of charged and uncharged sprays. The charged spray was applied with a hand-held electrostatic spinning disc sprayer and uncharged spray with spinning disc sprayer and standard knapsack sprayer with hydraulic nozzle. Fluorometric analysis was followed for quantifying tracer deposition at different elevations of the plant. Droplet density was observed with WSPs placed at different elevations of plant canopy. Electrostatic charged spray application was done with 3kV charging potential, 3500 – 4500 rpm spinning disc speed and 50 $ml.min^{-1}$ flow rate. The charging system provided CMR of 2.5 $mC.kg^{-1}$ approximately, with droplet size in the range of 115 – 140 µm measured by collecting droplet on MgO glass slide and analyzer. The result showed the deposition of tracer increased in 3.5 to 4.9 folds in rice crop with electrostatic spraying and 1.1 to 1.19 in soybean.

Bayat *et al.* (1994) conducted field experiment on comparison between spray depositions with conventional and electrostatically charged spraying in citrus trees for pest control. Investigations were conducted with code M_1 and M_4

with different configurations of spray application setups. The air carrier sprayer operated by standard PTO speed (540±10 rpm) was used with 2.3 mm orifice diameter nozzles with electrostatic charging system of 17 kV tension. The spraying was done at 3.5 $km.h^{-1}$ travel speed and deposition analysis was carried through fluorescent tracer, WSPs and fluorometric analysis. The relative deposition was calculated by equation,

$$RD = \frac{MS}{AS/LAI} \times 100$$

Where,

RD = Relative Deposition (%),

AS = Ideal Deposition ($\mu g.cm^{-2}$),

MS = Mean Stardust deposition determined by filter papers ($\mu g.cm^{-2}$),

LAI = Leaf Area Index (dimensionless).

The results showed that, the electrostatic application reduces losses in citrus trees by 11.6 per cent to 29.5 per cent, than the conventional spray application.

Wang *et al.* (1995) investigated the effects of operating pressure and nozzle height on uniformity of spray distribution pattern under laboratory conditions using five types of TeeJet^{R} 11004 nozzles. Nozzles were operated over three different heights (45.7 cm, 38.1 cm and 30.5 cm) and three different operating pressures (138 kPa, 276 kPa and 414 kPa). The results showed that effect of nozzle height on distribution uniformity was significant for nozzle height 30.5 cm to 45.7 cm. The results seemed to agree with manufacturer's recommended nozzle heights i.e. 38.1 cm to 45.7 cm with test data. However, effect of operating pressure found to be insignificant on distribution uniformity.

Sumner *et al.* (2000) conducted field experiments for comparing different spray techniques for pest management in cotton. Experiments included spray methods as air assisted spray, over the top hydraulic nozzle plus drop nozzles, electrostatic air assisted spray, over the top hydraulic nozzles and over the top plus shielded drop nozzles. Water sensitive cards and Leaf-wash method was used

to quantify the droplet deposition in various techniques. WSPs were placed into the canopy, top side and middle portion of canopy on both upper and undersides of leaves. Results have shown that electrostatic air assisted spray technique provided better coverage and lowest standard deviation in spot diameter (77 µm and 60 µm for top and underside resp.) than other methods.

Kirk *et al.* (2001) evaluated performance characteristics of aerial electrostatic spray system with different fields of cotton for control and management of *Ball weevil* and *Whitefly*. The prototype was studied at laboratory on the basis of commercial version of aerial electrostatic spraying system. Charge to mass ratio was assessed for corresponding flow rates, spray mixture and pest mortality. The prototype aerial electrostatic spray charging nozzle system was mounted on Cessna T1888C Ag-Husky, agricultural aircraft (231 kW, 12.74 m wingspan), calibrated for 9.4 lit·ha^{-1} at 483 kPa and conventional spray system calibrated for 46.8 lit·ha^{-1} at 193 kPa. Spray droplet deposits with Caracid brilliant flavine dye were collected with six water sensitive papers per plant at random locations and quantified by dye fluorometry. They found higher pest mortality in electrostatic aerial spray as 96.60 percent compared to conventional spraying with 76.60 percent pest mortality.

Laryea and No (2002) investigated the spray characteristics of charge injected electrostatic pressure swirl nozzle for oil burner for agricultural product drying. Experiments were conducted with direct nozzle charging of hydrocarbon fuel with negative polarity. A point sharpened tungsten wire with 1.0 mm diameter was used as an electrode and placed concentrically inside fuel supply pipe. Fuel injection pressures ranging between 0.7 to 0.9 MPa with flow rates between 69.0 to 77.6 ml·min^{-1} were used. The electrode was connected to variable DC high voltage from -4 to -12 kV and Faraday pile connected with digital electrometer was used to collect spray charge. Experiments reported that electrical breakdown occurred at -10 kV at injection pressure lower than 0.9 MPa; while at injection pressure equal to 0.9 MPa electrical breakdown of fuel occurred at -12 kV.

Tong-Xian *et al.* (2004) conducted experiments on spray deposition over plant foliage with self-adhesive paper targets. Self-adhesive paper micro-slide labels were used as the targets to evaluate spray coverage on tomato and citrus plant foliage. On both, upper and under leaf surfaces, self-adhesive papers were pasted randomly throughout the plant canopy before spray application. The spray solution was consisted of Brilliant blue dye (FD&C No.1) as a tracer in aqueous base. The tracer dye deposited on labels was then subsequently eluted into vials of water (20 ml) after spray application and the concentration of the rinsate obtained therefore was determined by spectrophotometry. Also the spray coverage was evaluated for comparison with same sized WSPs stapled onto the leaves. Comparatively more dye was recovered from labels than the actual plant leaves and recovery by two methods was correlated using yellow WSPs i.e. r-value = 0.83 to 0.99. Dye recovery was also correlated with the coverage measured using WSPs i.e. r-value = 0.72 to 0.95.

Latheef *et al.* (2008) conducted experiments on aerial electrostatically charged sprays to find its efficacy against fruitfly on cotton. Cessna AgHusky Agricultural aircraft equipped with spray boom was used for the application with 1.5 to 2.0m boom height above the crop canopy. The spray boom was engineered to achieve application rate of 4.68 $lit.ha^{-1}$ and assembled with 82 and 32 nozzles at 482.7 kPa and 193 kPa operating pressure respectively, with bipolar charging system of +5 kV potential. Six leaf samples were collected after application from top and mid-canopy locations randomly from the plot and tracer deposition was measured with Turner Digital Fluorometer (Abbott Diagnostics, C.A.) in terms of $ng.cm^{-2}$. They observed that there was no significant difference between charged and uncharged sprays.

Barbosa *et al.* (2009) conducted study on deposition and canopy penetration of different sprays in soybean (Glycine Max-L). Artificial mylar cards and tartazine tracer were used to quantify the distribution and penetration performance. The equation used for converting sample concentration results in units of volume per unit area was,

$$Deposit = \frac{C \times V}{\rho \times A}$$

Where, 'Deposit' is the final concentration, 'C' is the tracer concentration obtained through laboratory analysis (mass.lit^{-1}), 'V' is the solvent volume, 'ρ' is the original concentration of solution (mass per unit volume) and 'A' is the target surface area. Multiple comparisons on means were made using Fisher's Test of Least Significant Difference (LSD).

Celen *et al.* (2009) studied the effect of air assistance on deposition characteristics of tunnel type electrostatic sprayer. The sprayer was attached to a 55 kW tractor and having 0 to 17 kV power supply unit with 12 V DC input. Vineyard sprayer having 50 l.min^{-1} discharge rate at 2 bar pressure and operated on crop position of 3 m × 1.5 m and 1.2 m height. Air support system was used having 710 mm diameter fan and air flow rate of 600 l.min^{-1} at 36 m.s^{-1} air velocity. Tetrazine food dye was used as a tracer. Deposition was increased by 7.8 % with air support and 23.5 % reduction in drift.

Jaworek *et al.* (2009) conducted study on electrostatic spraying of nano-thin films on metal surfaces. The electro-spray system was consisted of stainless steel (SS) capillary nozzle and heated stainless steel table of 120 mm diameter. The distance between nozzle tip and the table was kept 15 mm and 25 mm. The substrate was SS rectangular plate of 500 µm thickness and 25 mm x 30 mm dimensions. The solvent was evaporated from the spray solution by providing an electric heater placed beneath the table. The nozzle was connected to the HVAC-DC generator Model-P04015 TREK, switched to positive polarity while plate and the extractor were grounded. The spray plume was recorded using CCD Camera Model-NG-VS400, Panasonic Inc. Methanol was used as the solvent and MgO particulates of size 100 nm as solute. The DC bias was in the range of 5.7 to 6.3 kV and AC in 1.5 to 4.0 kV at liquid flow rate of 1.5 ml.h^{-1}. The results showed homogenous metal-oxide films on substrate of thickness 1 – 2 µm.

Mishra *et al.* (2014) conducted performance evaluation of electrostatic spraying in orchards with USA made ESS-MBP electrostatic sprayer. Tests were

carried out with various experimental combinations of WSPs mounted on leaf top and leaf underside at distinct portions of plant canopy as top, middle, bottom and dense parts. Droplet density and uniformity coefficient for corresponding portions were obtained with the help of PC-assisted Stereo zoom microscope CCD camera and compared between electrostatic (single and twin nozzle) spray and conventional non-electrostatic spray. They found that average droplet density on upper and underside of leaves was substantially higher in charged spray i.e. 57.53 percent and 59.60 percent respectively than uncharged spray method.

2.5 Measurement of Spray Droplet Size

Derksen and Bode (1986) conducted study on droplet size analysis to determine suitable sampling techniques and atomization characteristics of selected rotary atomizers. Measurements of drop size and the size distribution were done using OAP-260X Laser Imaging Probe by Particle Measuring Systems, Inc. The atomizers were operated at rotational speeds 1000 to 5000 rpm and flow rates from 0.07 to 2.95 lit.min^{-1}. The data was analyzed using computer program DROPSZ. The drift potential of the sprays produced by all atomizers at 2000 rpm was very low over entire range of flow rates and resulted droplet size was in the range of 100 to 345 µm.

Krause and Derksen (1991) conducted comparison experiment between Hand-gun type electrostatic sprayer and Cold-fog sprayer in a production greenhouse. Spray distribution characteristics and penetration data were assessed and analyzed under cold-field emission scanning electron microscope (CFESEM) with energy dispersive X-ray analysis system. The spray treatment was done on 2 month old *Fucshia spp.* randomly placed in a commercial greenhouse. The spray applied by ESS's electrostatic sprayer was 9 litres, while it was 20 litres for the same greenhouse by cold-fog sprayer. Droplet size observed for the electrostatic sprayer was in the range of 5 – 80 µm and 50 – 200 µm for cold-fog sprayer respectively. As compared to the cold-fog sprayer, electrostatic sprayer showed more deposition with better uniformity, better canopy penetration and uniform droplet size.

Almekinder *et al.* (1992) investigated spray deposition patterns of an electrostatic atomizer replying primarily on electrostatic and gravitational forces for transportation and subsequent deposition. The wind-tunnel experiment was conducted for electrostatically charged sprays on artificial plants. TotalStat Electrostatic atomizer was used for charged spray application and two Aluminium bars (grounded) 50 cm long and 2 cm O.D. were placed along each side of the atomizer to intensify electric field. The air pressure was maintained at 70 kPa and droplet size was measured with the help of Malvern 2600C Particle size analyzer with 300 mm lens. The charge to mass ratio was obtained from constructed Faraday's cage consisted of two metal pans and concentric rings. Spray cloud current was measured with Keithley Electrometer (Model-220 equipped with decade shunt). Charged spray applications were conducted with three charging voltages as 20, 25, 30 kV and resulting CMR was observed in the range of 0.4 to 8.0 $mC.kg^{-1}$. WSPs were used for studying deposition density and deposition pattern analyzed with microscope and calculated by software program FLUENT. The results showed that, CMR decreased with increase in droplet size (VMD) and liquid flow rate. The optimum droplet size was observed in the range of 100 to 278 µm.

Bouse (1994) analyzed the droplet size for different types of aerial spray nozzles in an air-stream to simulate the operation on an aircraft. A laser imaging spray droplet spectrometer probe was used to measure the droplet size and determined the effects of spray pressure, air velocity and nozzle orientation on droplet size for solid stream, disc core, hollow cone, swirl type hollow cone, elliptical orifice fan type and deflector fan type nozzles. He concluded that, the spray pressure for solid stream nozzles oriented to the air-stream reduced the relative velocity and increased the droplet size.

Khadir *et al.* (1994) conducted studies on spray penetration through plant canopy and deposition characteristics of an air-jet assisted charged spray in wind tunnel. Air-jets with velocities of 0, 10, 13 and 16 $m.s^{-1}$ through a long 5.1 cm wide slot were used with 119 µm charged sprays. TotalStat Electrostatic atomizer

was used to atomize the spray with 36 kV voltage potential. The charged spray conveyed with an air-jet velocity of 16 $m.s^{-1}$, deposited significantly more spray on the targets than the charged spray without air assistance.

Sidahmed (1996a) developed theory of predicting size and velocity of droplets from pressure nozzles. It was postulated that atomization can be explained by energy balance equation for small mass 'Δm' of liquid separated from liquid sheet into a single droplet. When viscosity is negligible, the minimum droplet size diameter (d_{fmin}) associated with the Weber's number (N_{we}) and Bond's number (N_{bo}) and while surface tension is negligible d_{fmin} is associated with Reynolds number (N_{re}) and d_{fmax} is associated with '$N_{bo}.N_{re}/N_{we}$'

Sidahmed (1996b) conducted study on prediction of droplet size (D) from the flat liquid sheet with velocity (U_L) sprayed in an air-stream of velocity (U_A) and developed a mathematical model for predicting droplet size. As the existing theoretical equations based on aerodynamic instability and fail becomes infinitely large as U_A approaches U_L, restricted their suitability. Two empirical equations were developed, when U_L = constant and U_A = variable at water spray pressure 276 kPa, was represented by a regression line with coefficient of determination R^2 = 0.9977 and standard error of estimate (SEE) = 8.89.

For constant U_L and varying U_A,

$$D = D_{max} e^{|1-\frac{1}{U}|^n Ln\,(\frac{Do}{Dmax})}$$

For constant U_A and varying U_L,

$$D = D_{max} e^{|1-\frac{1}{U}|^m Ln\,(D_{Lo}/Dmax)}$$

The results showed good fit between experimental data and developed equations.

Johannama *et al.* (1999) conducted experiments on two fluid concentric internal mixing induction charging nozzle suitable for electrostatic spraying. Droplet size measurement was done with the help of Malvern 2600 Laser Scattering instrument at horizontal as well as vertical traverse. Volume Median Diameters were determined for both charged and uncharged sprays. The results

showed larger VMD in charged spray as compared to uncharged one, at three distinct operating pressures 0.14, 0.21 and 0.28 MPa and at spray liquid velocity 3 $m.s^{-1}$ and air velocity 30 $m.s^{-1}$. For charged sprays VMD obtained was in the range of 40 to 75 µm, while for uncharged spray it was in between 12 to 32 µm. The experiment also confirmed that there was a negative pressure created near centre of the nozzle which siphoned out spray liquid and helped for atomization too.

Fritz *et al.* (2009) evaluated a series of flat fan spray nozzles at different speeds and pressure combinations in a laboratory to study the deposition and droplet sizing characterization. The nozzle operating pressure was regulated and could be varied between 0 to 830 kPa with provided nozzle traverse speed between 0.5 to 7.0 $m.s^{-1}$. Photoelectric Sensor system was used for positioning of nozzle and speed calculations. Three-way solenoid valve and photorefractive micro-sensor controlled the traverse of the nozzle. Desktop computer with CIO-DIO24-CTR3 interface card (Norton, Mass.) was used to control spray table operation. Depositional characteristics were evaluated using WSPs (Spraying Systems, Wheaton, Ill.) yellow of 26 x 76 mm size arranged on a suspended table surface. The treated WSPs were then scanned under Droplet-Scan^{R} (Version 2.2) software to determine droplet spectra (VMD and NMD). The results showed that there was increase in droplet size at higher application rates due to overlapping in the range of 47 – 87 per cent and from the single replication a jump from 249 µm to 602 µm VMD was observed in the image analysis.

The method of Electrostatic induction charging (EIC) system has no direct contact with the working fluid, the chances of getting high voltage shock to the operator are negligible and the power consumption is also considerably lower than the other methods. The method was selected for the study due to its best suitability for charging agricultural spray liquids.

CHAPTER III
MATERIALS AND METHODS

The methodology adopted for development of a prototype electrostatic induction spray charging system as an attachment to an existing powered knapsack mist blower, experimental setup made to evaluate the prototype for depositional characteristics and the protocol followed for its evaluation and data acquisition are detailed in this chapter.

3.1 Principles of electrostatic induction spray charging system

The method of electrostatic induction spray charging was adopted for this study by considering its known advantages over other charging methods such as high charge transferability, less hazardous to life and simplicity in construction. Fig. 3 illustrates the schematic arrangement of the components and working principle of an electrostatic induction spray charging system which has been adopted.

The system consists of a spray nozzle and electrode placed in the vicinity of spray atomization zone concentrically with the spray nozzle. When sufficiently high voltage DC potential is applied to the charging electrode and the spray liquid is grounded, an electrostatic field will be created around the electrode. The position of the electrode is fixed in such a way that it will be exposed to the maximum spray atomization area. According to Gauss's Law, the maximum droplet charging occurs when the droplet formation zone is exposed to the maximum field strength. Therefore, for any liquid having non-zero electrical conductivity, an excess image charge will be accumulated on the grounded spray liquid with opposite polarity.

3.2 Development of electrostatic induction spray charging system

The design for an electrostatic induction charging arrangement for a conventional "duro mist" nozzle was conceptualized based on the available theoretical background of liquid particulate charging. Experimental prototypes of

induction charging nozzle attachment was developed to suit a knapsack mist blower.

3.2.1 Powered knapsack mist blower

The powered knapsack mist blower selected for the study (Plate 1) was OLEOMAC make AM 162 model with the following specifications.

Power	:	4.5 HP, 3.3 kW
Displacement	:	61.3 cm^3
Max. air flow	:	20.0 m^3 min^{-1}
Air speed	:	70 to 90 m s^{-1}
Liquid delivery rate	:	0.67 – 5.00 L min^{-1}
Liquid tank capacity	:	16.0 L
Weight	:	11.5 Kg

3.2.2 Development of voltage amplification unit for HVDC supply

For charging an aqueous spray electrostatically, a high voltage DC power supply is essential. The basic voltage amplification unit mainly consists of a diode pump voltage multiplier. It has a special arrangement of P-N junction diodes and capacitors with an alternating current input. The voltage amplification depends upon the number of stages of diode and capacitor ladder and the capacitance value.

3.2.2.1 Voltage Inverter Circuit

In order to convert input DC voltage from battery into an amplified AC voltage, an inverter circuit is necessary. It consists of a pulse generator and a high voltage transformer, in which the input DC voltage is converted into a pulsating square wave signal through the pulse generator circuit. This pulsating voltage is applied across the primary winding of the high voltage transformer, which then generates a sinusoidal alternating wave in the secondary winding due to mutual induction. This AC voltage can be used as an input source for the voltage amplification circuit.

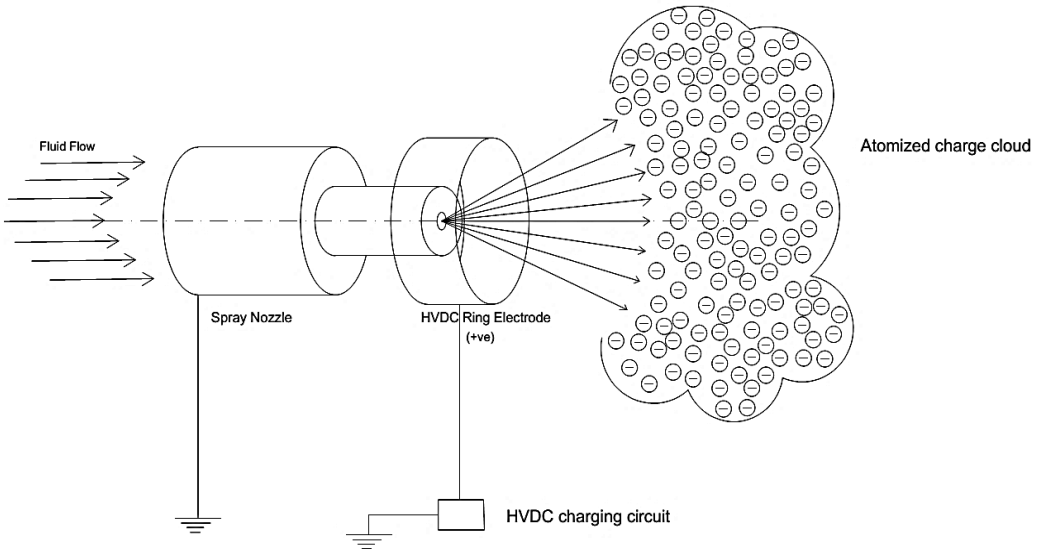

Fig. 3. Electrostatic induction spray charging system

Plate 1. Powered knapsack mist blower

3.2.2.2 Diode-Pump Rectification

A diode-pump rectifier circuit was developed as shown in Fig. 4. The figure illustrates the arrangement of diodes and capacitors with an AC voltage input (V). The circuit doubles the voltage output with a cascade arrangement of two diodes and two capacitors. However, the practical output voltage shows slight reduction due to ripple in the voltage amplification. This voltage doubler or multiplier circuit generally known as the Cockcroft-Walton (C-W) voltage multiplier (Fig. 5). The theoretical output voltage could be calculated by the formula as,

$$V_{Output} = 2 \times N \times V_p$$

Where,

V_p = Peak value of voltage supply

N = Number of capacitors in the circuit

The practical voltage output differed slightly from the output voltage calculated theoretically due to the ripple effect in voltage amplification. Then it could be expressed in terms of Ripple voltage (V_R),

$$V_R = \frac{I \times N(N+1)}{2 \times C \times F}$$

Where,

I	=	Load current, A
N	=	No. of capacitors
F	=	Driving Frequency, Hz
C	=	Capacitance, farads

Considering the alternating sine wave input, the lower rectifier causes the series capacitor to charge to the peak voltage of the input wave form. This occurs during the negative going excursions of the wave form and during positive going half-cycle, the charged capacitor and the transformer become effective in the series. This series arrangement charges the output capacitor to the sum of these two voltages and in turn, become equal to the twice of the peak value of the transformer voltage.

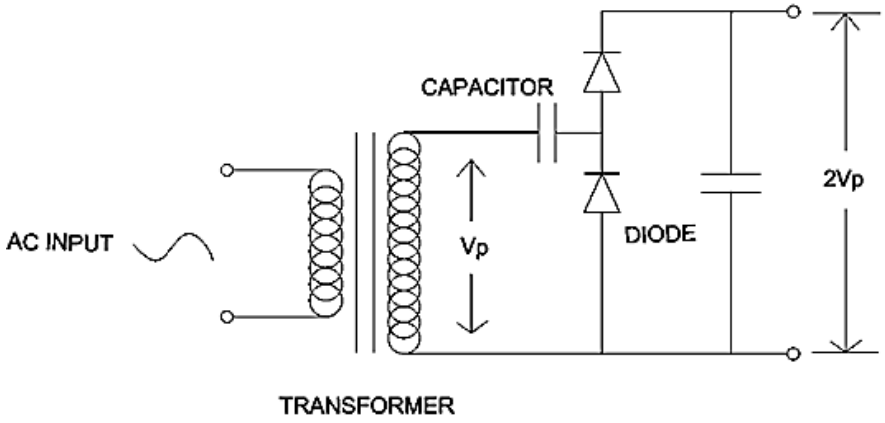

Fig. 4. Diode-Pump Rectifier

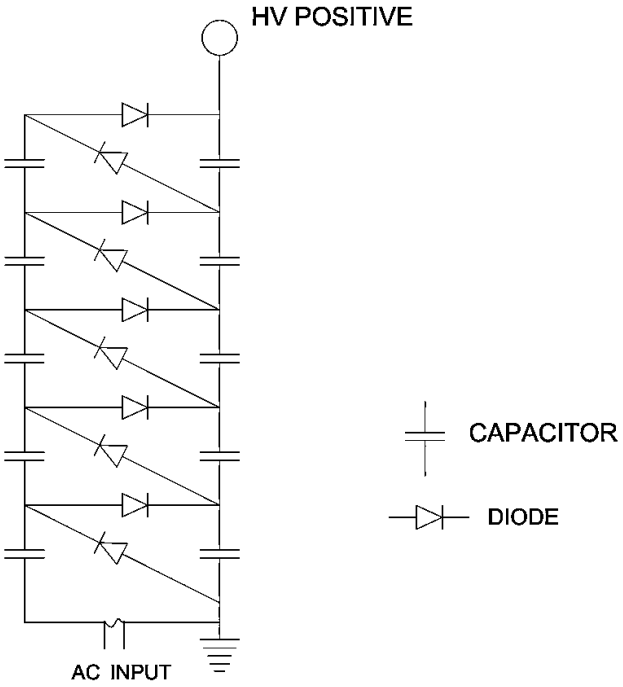

Fig. 5. Cockcroft-Walton voltage multiplier

Fig. 5 illustrates the further arrangement of multiple numbers of the cascade stages of the C-W voltage multiplier for higher output voltages with required polarity.

iii. High Voltage generator

A high voltage generator was fabricated on the basis of Cockcroft-Walton voltage multiplier principle, using 6 V DC battery with 0.25 mA current as an input source. It consisted of a high voltage transformer with different stages of cascade multiplier having IN4007 diodes and 3 kV ceramic capacitors (1.8 µF). A total five numbers of HVDC generators were fabricated (Fig. 6), so as to get an output voltage of 1000 V, 2000 V, 3000 V, 4000 V and 5000 V. As the voltage-multiplier circuit requires an AC input, an inverter circuit was introduced in between the DC input battery and the high voltage transformer. The pulse generator in the inverter circuit was fabricated with NE555 standard timer Integrated Circuit and two 3296-Electronic Potentiometers to adjust the duty cycle and frequency (Plate 2).

The whole HVDC generator unit was accommodated in an insulated box to avoid arcing, direct contact with the operator or with any other conducting materials to avoid any sort of casualty.

3.2.3 Development of High Voltage Electrode Assembly

For inducing the high voltage generated by the HVDC generator, a suitable electrode assembly with three distinct designs of electrode positions was developed, as Model-I Exposed Electrode assembly.

3.2.3.1 Model I : Exposed electrode assembly

The Fig. 7a and Fig. 7b illustrates geometry of the designed and fabricated HV-electrode assembly with the radial distance of electrode at 1.5 to 2.0 cm from the centre point of spray nozzle. The material for fabricating the assembly was selected on the basis of proper insulation as well as machinability, hence the Cast-Nylon-6 circular section rod of 75 mm diameter was used.

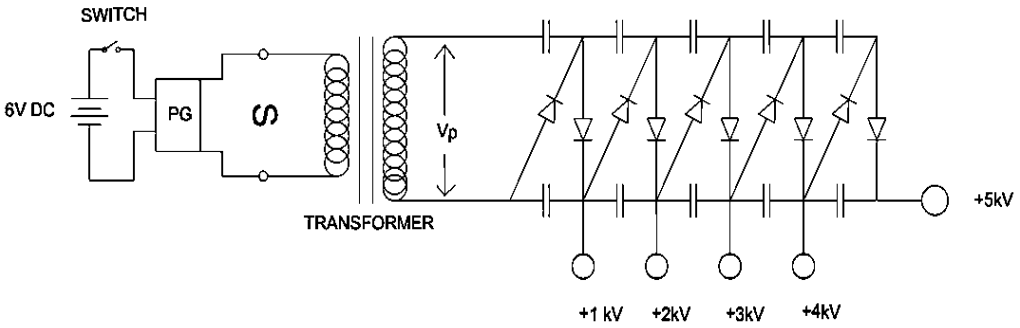

Fig. 6. High Voltage generator

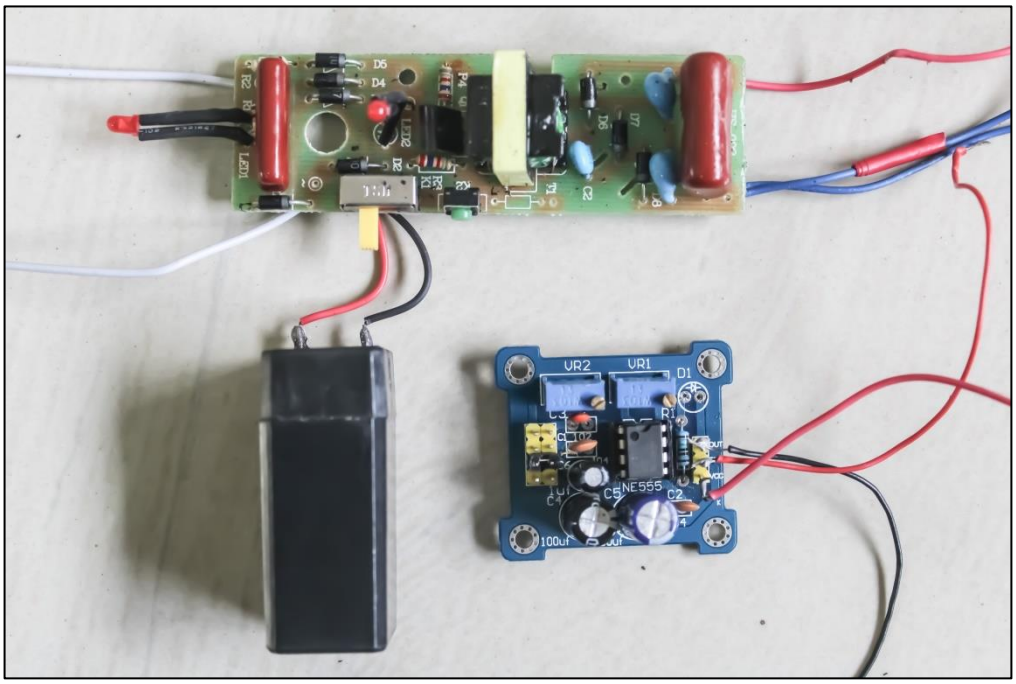

Plate. 2. High Voltage generator with pulse generator

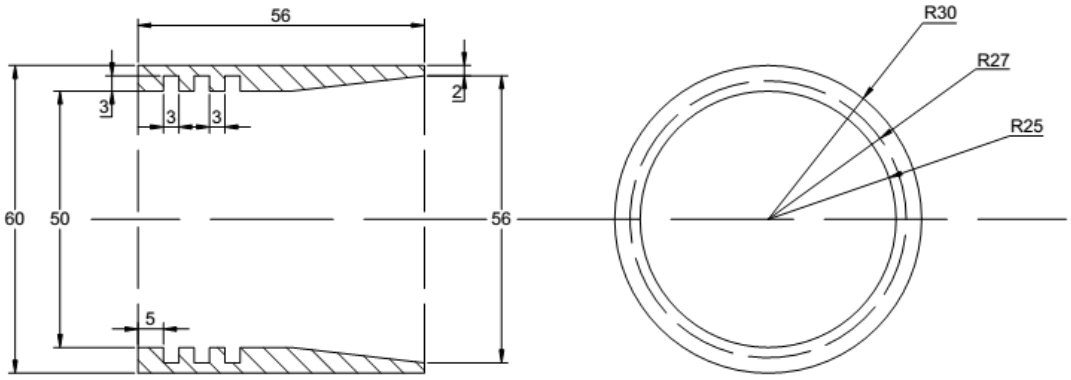

Fig. 7a. Model I : Exposed electrode placement assembly (Sectional view)

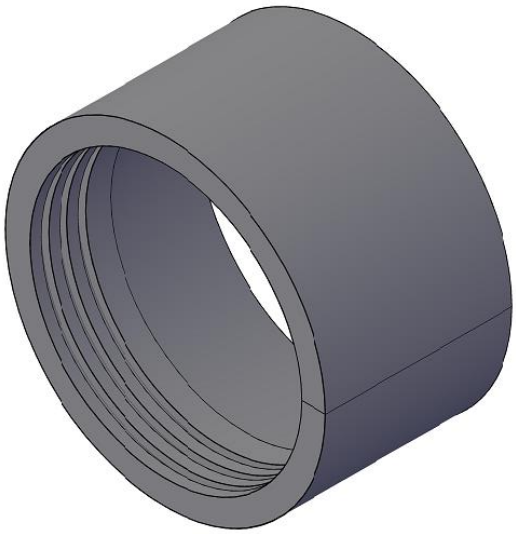

Fig. 7b. Model I : Exposed electrode placement assembly (Isometric view)

The electrode carrier was designed in such a way that, introduction of the electrode assembly to an existing system must not produce any type of hindrance in the air-flow generated by blower. A slope of 40 per cent was provided to the inner edge of the carrier to minimize the air-flow turbulence. Three slots of 2 mm × 2 mm (width × depth) with interspacing of 3 mm were provided internally from the outer end of the carrier, for placing the HV ring electrode.

3.2.3.2 High Voltage Charging Electrode

In order to get high electrical conductivity and low resistance losses as well as ease of workability, pure Copper wire of circular section with the diameter of 2 mm was selected as an electrode material. Copper wire has low electrical resistance with easy workability, which facilitates shaping it into desired manner. Fig. 8. shows the shape and dimensions of the HV-charging copper electrode used in the present study.

3.2.3.3 Existing Spray Head on the mist-blower

The geometrical details of an existing spray nozzle head installed on the mist-blower unit by the manufacturer were detailed in Fig. 9. This spray head was provided with the flanged disc shape with 20 nos. of discharge outlets of 2 mm diameter, radially around the periphery. This spray head was working on the gravity along with low head centrifugal pump driven by the engine shaft, delivering the radial spray jets into the air-flow generated by the centrifugal blower. The direction of the spray jets and the high velocity air-flow were right angles to each other, which caused the atomization of the spray fluid.

In this mechanism, the size of droplets formed was completely depending upon the velocity of the air-flow. These droplets were then carried away along with the high velocity of continuous air-blow. The developed charging system which consisted of HVDC charging circuit and electrode carrier assembly was fitted as an attachment to the existing engine operated knapsack mist-blower without any modification or alteration with the existing spray nozzle head.

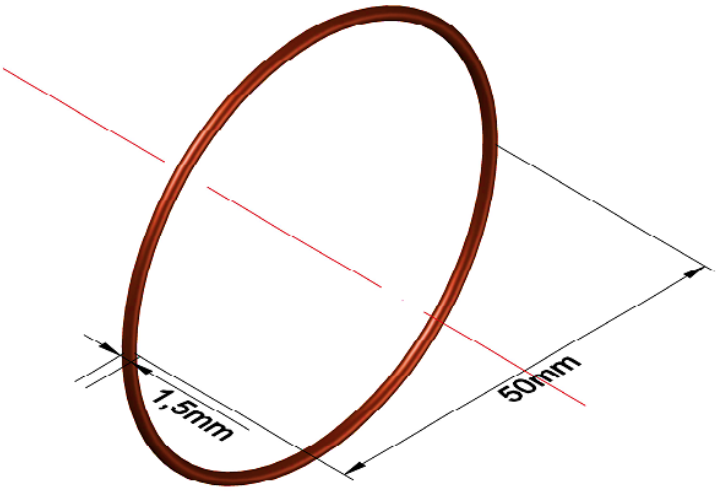

Fig. 8. HV-Charging electrode

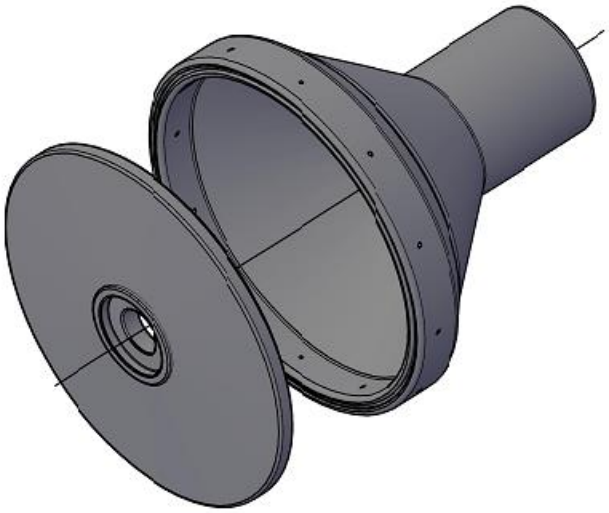

Fig. 9. Nozzle Assembly of the knapsack mist blower

3.3 Laboratory Experimental Setup

Measurement of high voltage, generated by the fabricated HVDC generator unit was one of the critical factors, since this high voltage was the basic parameter influencing the induction charging of spray. Similarly, the current induced in the spray was also an important factor in the induction charging, hence it has to be measured accurately. The most suitable and safe method for measurement of high voltages and current related with it, was using a High Voltage Probe in combination with a Digital Multimeter unit with the compatible data logger software. Also the Faraday's Cage was fabricated as per the requirements for the study to measure the charged spray cloud current.

3.3.1 Digital Multimeter unit

The digital multimeter Model No. KM-5040T/BM-812a of make KUSAM-MECO Brymen, Ind. Ltd. (Plate 3) was used for the measurement of voltage and current generated by the HVDC generator unit. The DMM was equipped with 5000 counts and analog bargraph screen and also enabled with RS-232 Computer Interface-Data Logging Software which can collect data from the DMM with Infrared serial bus cable at the data collection speed of one reading per second. Plate 4 shows the face window of the Computer Interface-Data Logging Software. The general specifications of the DMM used were,

Make	:	Kusam-Meco Brymen Industries Ltd.
Model	:	KM-5040T/BM-812a
Capacity	:	1000 V, 10 A max.
Sensitivity	:	0.1 µA, 10 µV
Accuracy	:	± 0.5 % (3 Digits)

3.3.2 High Voltage Probe

In order to measure the high voltage potential at the charging electrode in the range of kilovolts, a High Voltage Probe Model No. PD-28 of make KUSAM-MECO Brymen, Ind. Ltd. was used (Plate. 3), in compatibility with the DMM. High voltage probe was basically a voltage divider network consisting high resistances in series form. The high voltage was applied to the voltage divider

network and the corresponding current flowing through the low resistance was measured by the DMM, which has been calibrated to show corresponding high voltage. The high voltage probe used in the present study has the specifications as,

Make	:	Kusam-Meco Brymen Industries Ltd.
Model	:	PD-28
Capacity	:	40 kV DC or 28 kV AC max.
Input Impedance	:	1000 MΩ
Attenuation Ratio		1000 : 1
Accuracy	:	± 1 %

The HV-probe has an insulated hollow body with slender shape inside which, a voltage divider network of series high resistances have been connected. The tip of probe was pointed and made of brass, as the measuring contact surface to the high voltage terminal. At the base, insulated handle has been provided with the surge protector shield which assures the operator safety during measurement of such high voltages. Three cables emanated from the prob and serves as the earth and the other two for connecting DMM.

3.3.3 Faraday's Cage

The induction spray chargeability of the developed electrostatic induction spray charging system could be measured only by measuring the charge acquisition by the spray cloud. The charge acquired by the spray cloud is directly proportional to the charge induction capacity of the HV electric field produced around the electrode by the developed system. Faraday's Cage is one of the simple and accurate methods of measuring the spray cloud charge, in the laboratory (Law, 1975; Almekinder *et al.*, 1992). It could be fabricated in different shapes and sizes with different sensing elements according to the requirements of experimental setup, without violating the basic concept.

High Voltage Probe **Digital Multimeter**

Plate 3. High Voltage Measuring System

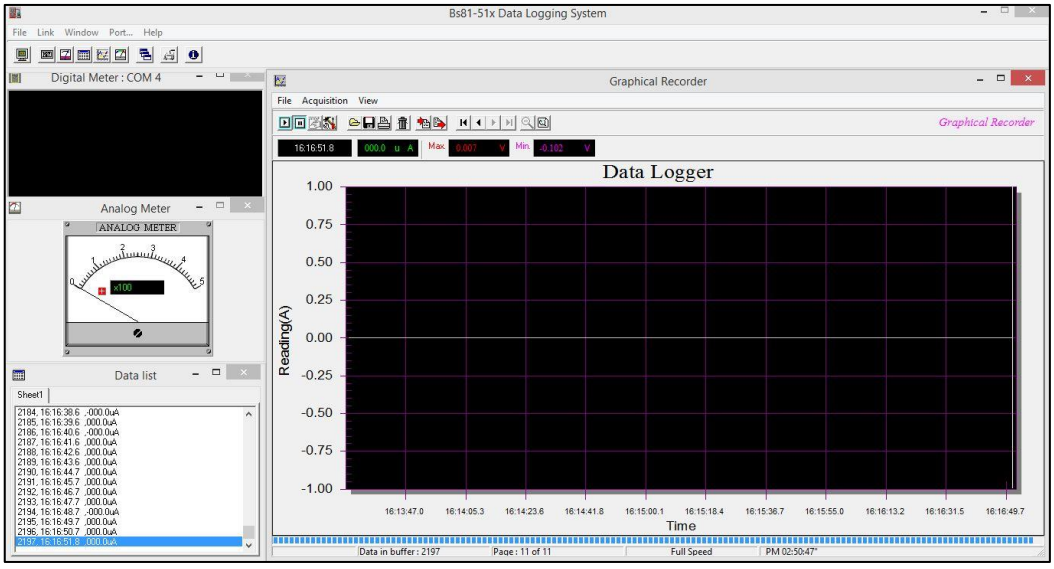

Plate 4. RS-232 Computer Interface-Data Logging Software

In this study, water was used as the spray fluid and it was required to measure the induced spray cloud voltage instantaneously. The Faraday's cage was designed with general thumb rules and fabricated accordingly with a Polypropylene vessel and Aluminium mesh, as illustrated in Fig. 10. The shielding Aluminium mesh was wrapped around the insulating vessel of cylindrical shape, keeping it in a horizontal position, to avoid atmospheric electric field interference to the charge collector mesh.

The charge collector Aluminium mesh was placed inside the vessel, vertically at marked intervals measured from the spray intake end of vessel (Plate 5). The cylindrical shape of the insulating vessel facilitated easy collection of spray intercepted by collector mesh, as the final outcome from the Faraday's cage was to get Charge-to-Mass ratio of the spray under test. CMR could be calculated from the charge collected from the spray and mass of intercepted spray. The connections were made between the Faraday's cage and Digital Multimeter enabled with Computer Interface Data Logging Software, as ground wire to the grounded shielding mesh and positive terminal to the charge collector mesh.

The charge induction on the spray cloud by the developed system was found to be very low, since the droplet size formed with the air assisted mechanism of spray nozzle was heterogeneous in size (500 µm to 1500 µm) even at blower operated in full engine throttle, giving maximum air-flow velocity (70 to 90 $m.s^{-1}$). The required droplet spectrum for effective induction charging was strictly 80 to 250 µm (Law and Cooper, 1988). Moreover, the dripping of spray fluid was also observed even at full throttle operation, thus lead to drop in the electrode potential.

3.4 Model II : Redesigned nozzle with reduced spray-jet outlets

A new nozzle liquid outlet was desisgned and fabricated based on geometry of the existing nozzle, with some modifications as detailed in Fig. 11. The number of spray-jet outlets were reduced from 20 to 6 and outlet diameter was reduced from 2 mm to 1 mm, keeping overall geometric shape similar to existing nozzle.

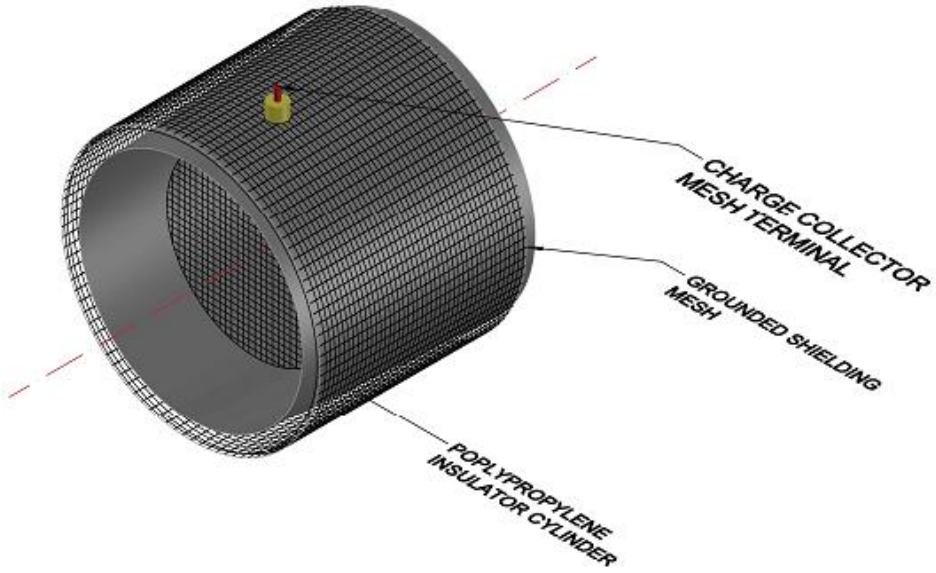

Fig. 10. Schematics of Faraday' Cage

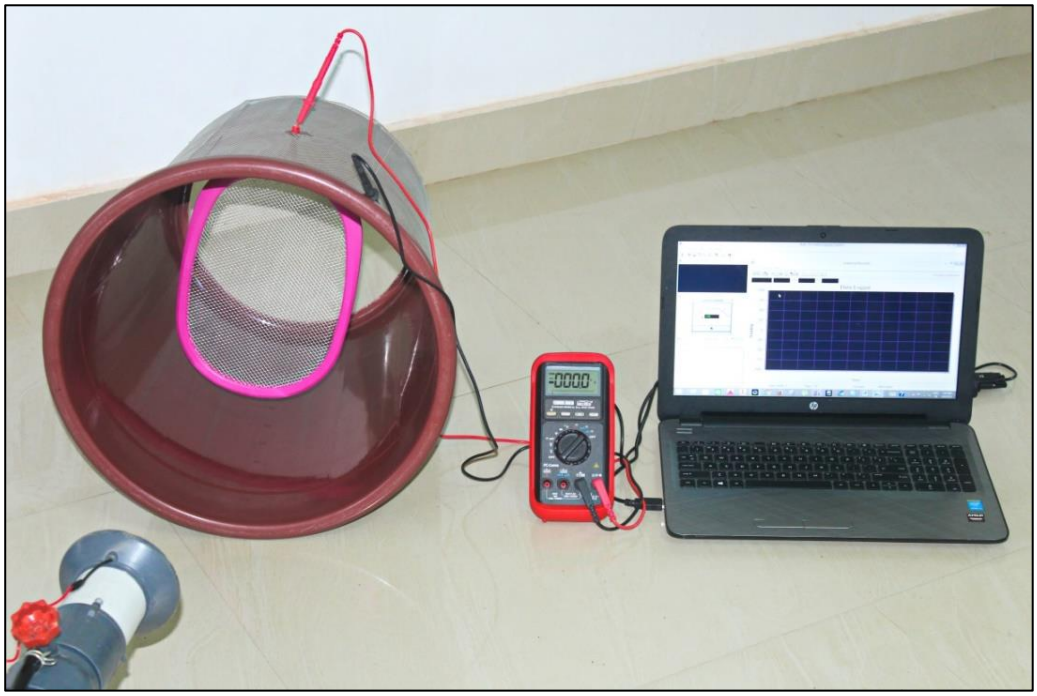

Plate 5. Faraday' Cage for spray cloud charge measurement

The angular spacing between two consecutive discharge points was increased from 18º to 60º for uniform distribution of spray fluid within the air-flow. However, no any significant improvement was observed from the operation of redesigned nozzle, as the dripping was still taking place with larger droplet size, though operated at full engine throttle. Therefore, a new type of spray nozzle was designed and fabricated to satisfy the study requirements.

3.5 Development of Self-Atomizing Hydraulic Nozzle

For getting required range of fine droplet size, an entirely different type of spray nozzle was designed and fabricated (Fig. 12, Fig. 13a and Fig. 13b), consisting a single orifice for fluid discharge with 0.10 mm opening diameter, working under hydraulic pressure ranging between 2.5 to 3.0 kg-cm^{-2}. The 12-24V DC operated low discharge high pressure diaphragm pump was selected to operate the nozzle, as it suited best for restricted space and corresponding addition in the gross weight of the whole equipment. The general specifications of the LD-HP Diaphragm pump used in the study were,

Make	:	Sea-Flo Pumps Ltd.
Model	:	SF25
Operating Current and Voltage	:	10 A, 12-24V DC
Output Pressure	:	2.5 kg.cm^{-2}

Nozzle was fabricated with Polypropylene material, provided with internal lateral entry of spray fluid towards the discharge point. The new design helped to get hollow-cone spray pattern with fine spray. The nozzle was operated separately with diaphragm pump and all the components were assembled together to form a single unit as Self-Atomizing Pressure operated nozzle type Electrostatic Induction Charging Knapsack Mist-Blower.

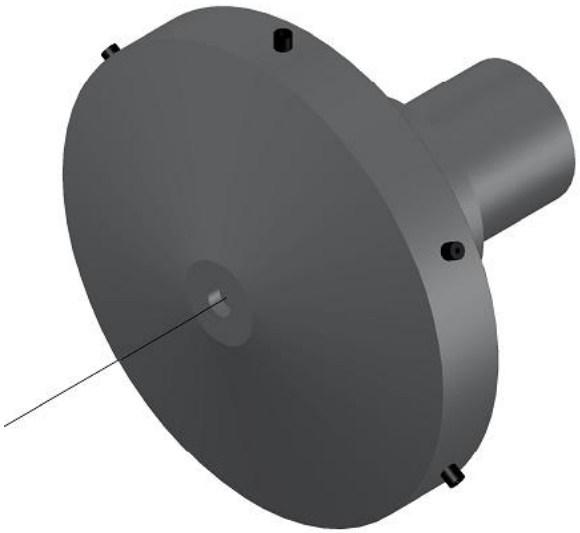

Fig. 11. Model II : Redesigned nozzle with reduced spray-jet outlets

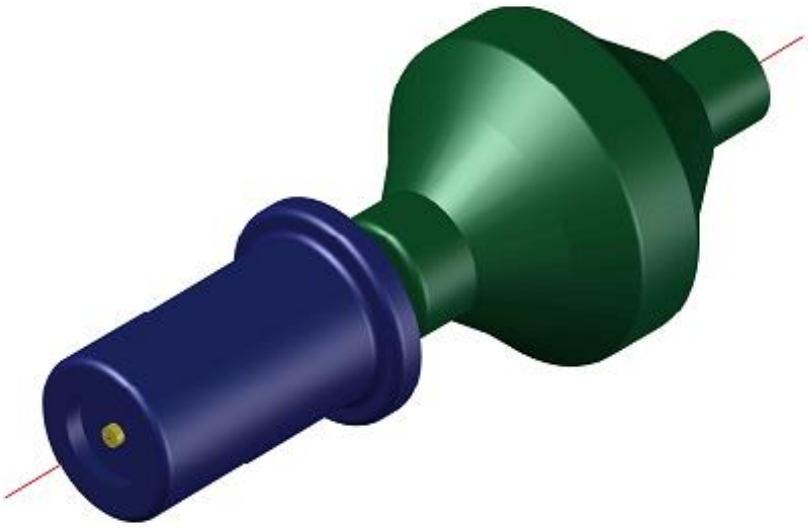

Fig. 12. Self-Atomizing hydraulic nozzle (Complete View)

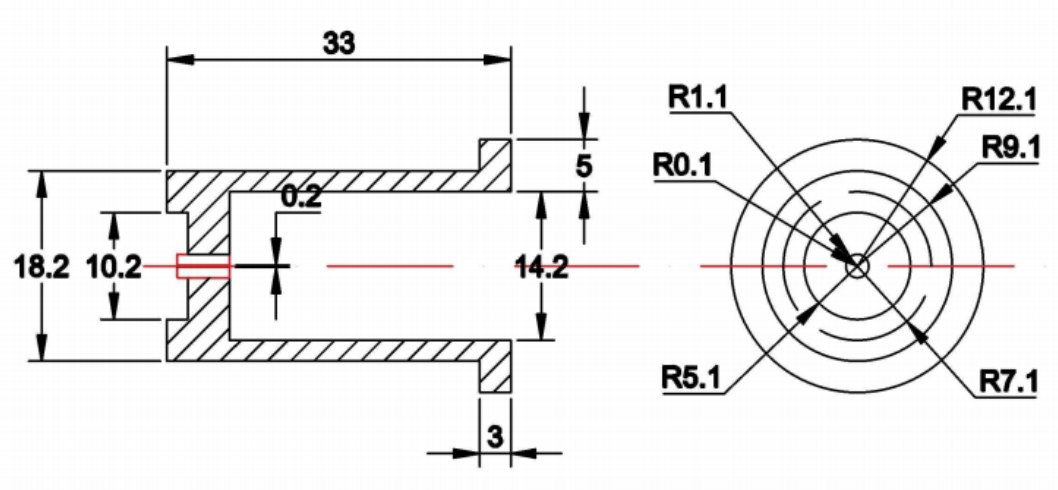

Fig. 13a. Self-Atomizing hydraulic nozzle (Sectional View)

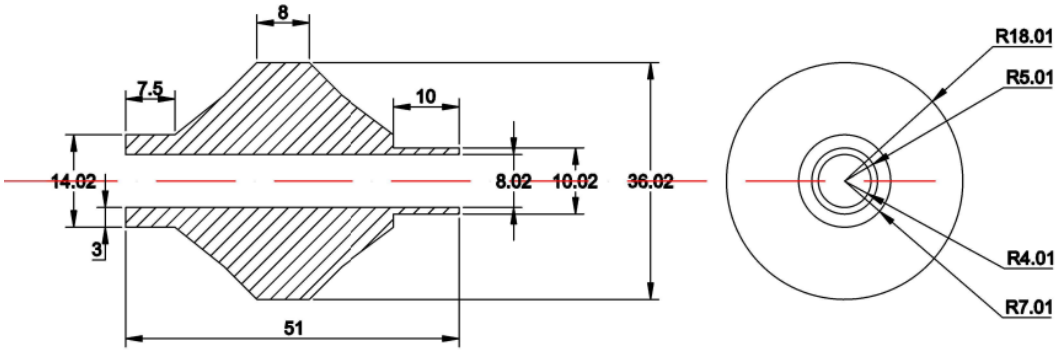

Fig. 13b. Adapter for nozzle fitment (Sectional View)

3.6 Model III : Exposed electrode assembly

The exposed high voltage induction charging electrode assembly as in Model I was installed for the new nozzle designed and fabricated. The electrode position was kept radially 25 mm away from the atomization zone, as the internal radius of the existing nozzle diffuser was 30 mm and to provide minimum air flow disturbance. Three different lateral positions (0 mm, 5 mm, 10 mm and 15 mm) of the electrode ahead of the atomization zone were evaluated.

Even though the model was capable of inducing charge to the spray droplets, the potential of electrode was reduced after a period of time of continuous operation due to shortage by the drops attached on it by wrap around effect of electrostatic spray. The deposition of chemicals due to wrap around effect over the electrode will lead to corrosion of electrode. Moreover frequent cleaning of electrode will lead to damage of electrical connections of the system as well as human hazards due to residual electricity present in the circuit. Hence the concept of embedded electrode system was materialised.

3.7 Model IV : Embedded electrode assembly

In this model, the copper wire ring electrode embedded in the carrier sleeve. The fabrication details of the prototype were same as detailed in section 3.4.3 with the electrode positioned as embedded with reference to the spray atomization zone. This design facilitated proper insulation of the charging electrode against wetting by tiny spray droplets. The wetting of electrode reduced the induction spray chargeability considerably. In this design also three slots were provided for placing charging electrode as provided, but externally over the periphery of the carrier sleeve (Fig. 14a and Fig. 14b).

3.9 Model V : Narrow embedded electrode assembly

In this model orifice diameter of the electrode carrier was reduced from 50 mm to 30 mm (Fig. 15a and Fig. 15b). This was done in order to bring the position of charging electrode radially closer to the spray atomization zone. Then the chargeability of spray droplets could be increased considerably than the other models.

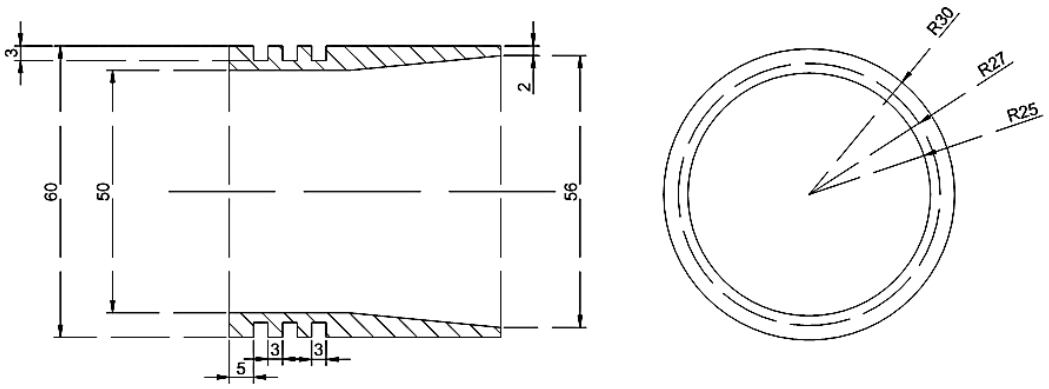

Fig. 14a. Model IV : Embedded electrode assembly – Sectional view

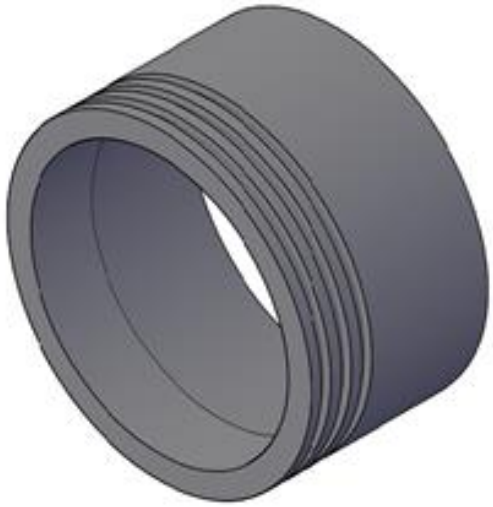

Fig. 14b. Model IV : Embedded electrode assembly – Isometric view

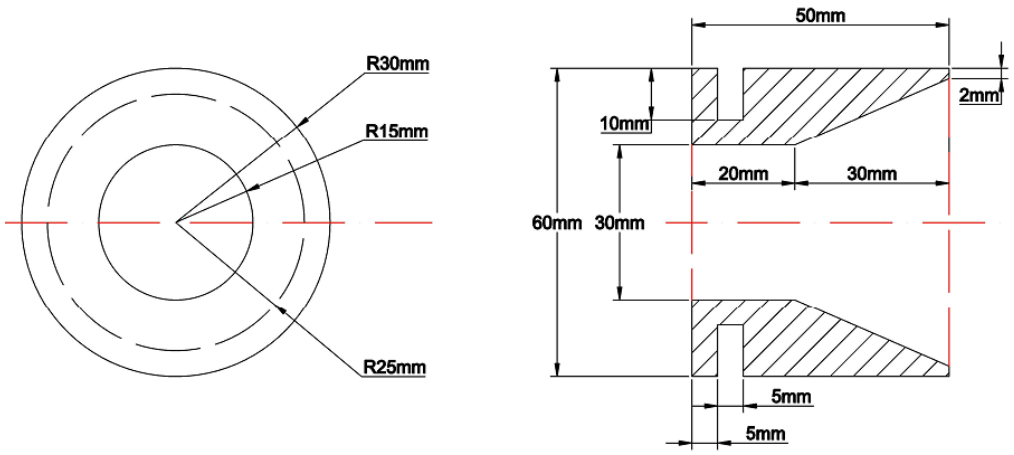

Fig. 15a. Model V : Narrow embedded electrode assembly (Sectional view)

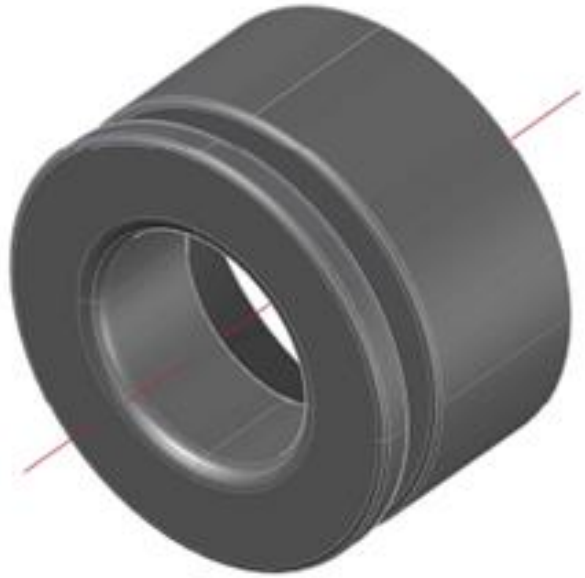

Fig. 15b. Model V : Narrow embedded electrode assembly (Isometric view)

The prototype of electrostatic induction charging unit attached to the powered knapsack mist blower (Plate. 6) was then evaluated under laboratory as per the specific experimental procedure.

3.10 Experimental Procedures

The different experimental procedures were followed with corresponding setups for measurement of charge induction over the spray cloud by developed HVDC generator and high voltage potential electrode and also for measurement of spray droplet size. The laboratory experimental setup for spray charge acquisition was as illustrated in Plate 7.

Model III

Voltage Potential : 1 kV, 2 kV, 3 kV, 4 kV and 5 kV

Electrode Position : 0 mm, 5 mm, 10 mm and 15 mm ahead of atomization zone

Model IV

Voltage Potential : 1 kV, 2 kV, 3 kV, 4 kV and 5 kV

Electrode Position : 0 mm, 5 mm, 10 mm and 15 mm ahead of atomization zone

Model V

Voltage Potential : 1 kV, 2 kV, 3 kV, 4 kV and 5 kV

Electrode Position : 0 mm, 5 mm, 10 mm and 15 mm ahead of atomization zone

Voltage carrying capacity : CMR was measured at 50 cm, 100cm, 150 cm, 200 cm and 250 cm from the nozzle

Model IV

Voltage Potential : 1 kV, 2 kV, 3 kV, 4 kV and 5 kV

Electrode Position : 0 mm, 5 mm, 10 mm and 15 mm ahead of atomization zone

Voltage carrying capacity : CMR was measured at 50 cm, 100cm, 150 cm, 200 cm and 250 cm from the nozzle

Model V

Voltage Potential : 1 kV, 2 kV, 3 kV, 4 kV and 5 kV

Electrode Position : 0 mm, 5 mm, 10 mm and 15 mm ahead of atomization zone

Voltage carrying capacity : CMR was measured at 50 cm, 100cm, 150 cm, 200 cm and 250 cm from the nozzle.

Plate 6. Electrostatic induction charging unit attached to the powered knapsack mist blower

Plate 7. Experimental Setup

3.10.1 Measurement of charge induction on the spray cloud

The charge induction was measured for the different experimental setups, as given below :

i. HVDC insulated wire electrode was mounted directly over the spray nozzle.
ii. Blower was operated at operating condition, so as to produce an air stream of velocity 60 to 70 m-s^{-1}.
iii. Faraday's cage was placed co-axially facing the air stream in front of spray nozzle at five different horizontal distances of 0.5 m, 1.0 m, 1.5 m, 2.0 m and 2.5 m.
iv. The charge induction was measured for five distinct voltage potentials of 1 kV, 2 kV, 3 kV, 4 kV and 5 kV at specific five longitudinal locations of the faraday's cage.
v. The charge induction was measured for each combination of charging potentials and distance of faraday's cage from the nozzle, with three replications for concordant values.
vi. The induced charge on spray cloud was measured with the help of DMM and computer based data logging software.

3.11 Measurement of Spray Droplet Size

The spray droplet size was measured at identical operating conditions since the spray chargeability was inversely proportional to the droplet size (Plate 8 and Plate 9).

Experimental Setup :

Bromide Photo paper of size 5 cm × 5 cm was used for capturing the droplet spectrum. Methylene Blue dye was used for pigmenting the spray fluid. Pigmented spray solution was prepared by dissolving 20 g of dry Methylene Blue dye in 1 litre of water. High resolution Scanner was used for scanning photo papers with 1200 dpi scan resolution. Computer based image analysis software Image-J-2016, Version 1.37.1 was used to analyse the scanned images and spectrum.

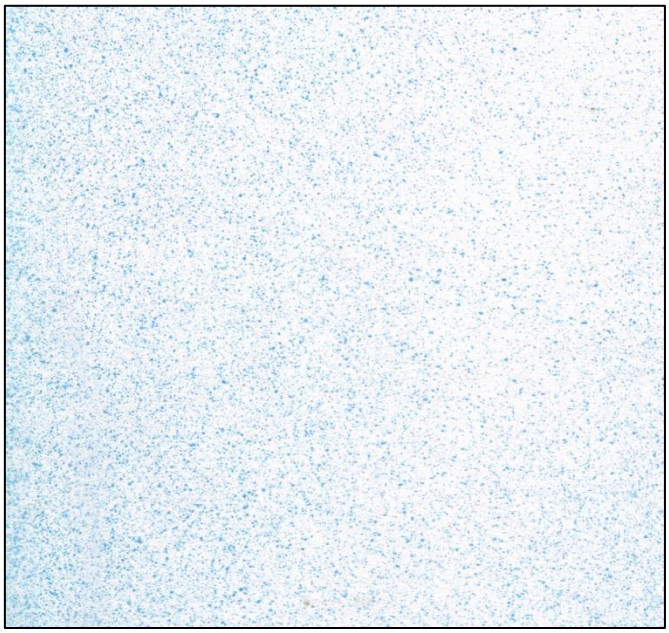

Plate 8. Spray impinged Bromide paper

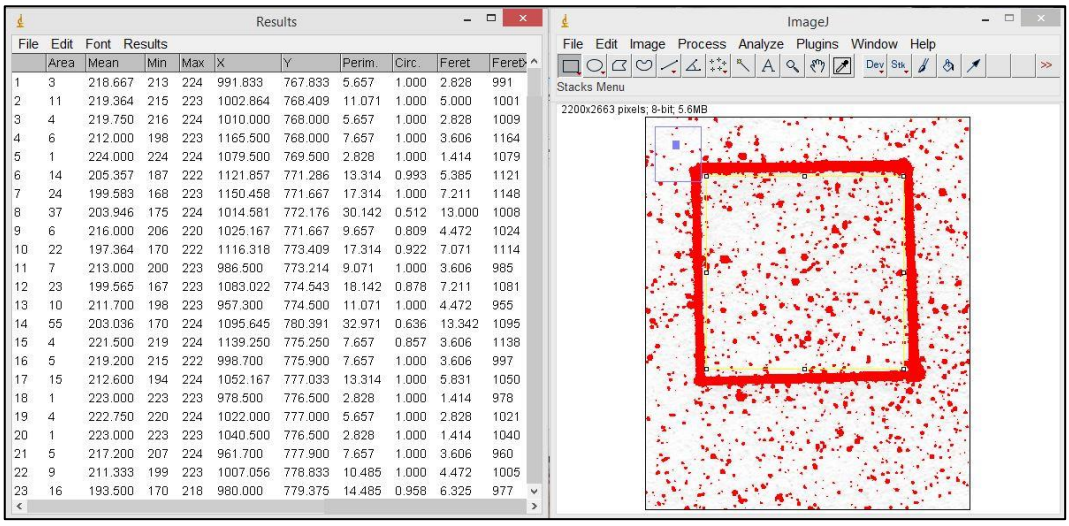

	Area	Mean	Min	Max	X	Y	Perim.	Circ.	Feret	Feret
1	3	218.667	213	224	991.833	767.833	5.657	1.000	2.828	991
2	11	219.364	215	223	1002.864	768.409	11.071	1.000	5.000	1001
3	4	219.750	216	224	1010.000	768.000	5.657	1.000	2.828	1009
4	6	212.000	198	223	1165.500	768.000	7.657	1.000	3.606	1164
5	1	224.000	224	224	1079.500	769.500	2.828	1.000	1.414	1079
6	14	205.357	187	222	1121.857	771.286	13.314	0.993	5.385	1121
7	24	199.583	168	223	1150.458	771.667	17.314	1.000	7.211	1148
8	37	203.946	175	224	1014.581	772.176	30.142	0.512	13.000	1008
9	6	216.000	206	220	1025.167	771.667	9.657	0.809	4.472	1024
10	22	197.364	170	222	1116.318	773.409	17.314	0.922	7.071	1114
11	7	213.000	200	223	986.500	773.214	9.071	1.000	3.606	985
12	23	199.565	167	223	1083.022	774.543	18.142	0.878	7.211	1081
13	10	211.700	198	223	957.300	774.500	11.071	1.000	4.472	955
14	55	203.036	170	224	1095.645	780.391	32.971	0.636	13.342	1095
15	4	221.500	219	224	1139.250	775.250	7.657	0.857	3.606	1138
16	5	219.200	215	222	998.700	775.900	7.657	1.000	3.606	997
17	15	212.600	194	224	1052.167	777.033	13.314	1.000	5.831	1050
18	1	223.000	223	223	978.500	776.500	2.828	1.000	1.414	978
19	4	222.750	220	224	1022.000	777.000	5.657	1.000	2.828	1021
20	1	223.000	223	223	1040.500	776.500	2.828	1.000	1.414	1040
21	5	217.200	207	224	961.700	777.900	7.657	1.000	3.606	960
22	9	211.333	199	223	1007.056	778.833	10.485	1.000	4.472	1005
23	16	193.500	170	218	980.000	779.375	14.485	0.958	6.325	977

Plate 9. Window of Image-J-2016 software during droplet spectrum analysis

Procedure :

i. The sprayer blower was operated at optimum throttle for the developed nozzle to provide identical air-velocity during droplet size measurement.
ii. The bromide photo paper was exposed to the spray cloud for a fraction of second perpendicular to the axis of spray nozzle at three different distances viz. 1.0 m, 1.5 m and 2.0 m respectively.
iii. The treated photo papers were scanned for generating digital soft-images and were fed to the Computer based image analysis software – Image-J-2016.
iv. The soft-images were processed in order to analyse the droplet spectrum and the average range of droplet size was determined.

3.12 Deposition characteristics

The spray deposition was quantified in terms of deposition per unit leaf area sprayed, by Leaf-wash method, as explained below.

3.12.1 Leaf wash method

In leaf wash method leaf samples from treated plant targets were collected randomly and different parts of the plant surface. Dye residues were washed from the top side and under sides of the leaves separately. Dye solutions thus collected were evaluated for transmittance with a Spectrophotometer and compared with the calibration from known washed deposits to determine dye deposition on each samples.

3.12.1.1 Tracer Deposit Extraction

1.5 g of fluorescent tracer (DAY GLO type GT-15-N Fluorescent Blaze Orange dye) was dissolved in 1000 ml of water, making concentration of tracer liquid 1500 ppm. This concentration of tracer residue on the target was analogous to pesticide active ingredient of an actual spray solution. This facilitated a direct correlation of relative deposition efficiencies of the electrostatic versus conventional spraying techniques. After spray, the spray fluid deposited on water sensitive paper or leaf surface were retrieved and the dye was extracted by washing with known quantity of double distilled water.

3.12.1.2 Measurement of Absorbance

The recovered tracer concentration was analysed for optical density (absorbance) with Spectrophotometer. Spectrophotometer was pre calibrated with double distilled water representing zero absorbance reading. Then further calibration was carried out in the visible region of the electromagnetic spectrum of wave length (λ) 555 nm, which is same as that of fluorescent tracer material and commercial agricultural chemicals. Solutions of known standard concentrations (ppm) of the tracer were prepared and measured for their optical density on the spectrophotometer. The concentration of the tracer of the sample was directly measured by the spectrophotometer in terms of ppm.

3.13 Statistical Analysis

The Completely Randomized Design (CRD) with General Linear Model (GLM) multiple comparisons Single Factor ANOVA were done to determine whether the difference between the performances of developed models were significant. The three developed Models (III, IV and V), charging voltages (1kV, 2kV, 3kV, 4kV and 5kV), Electrode placements (0 mm, 5 mm, 10 mm and 15 mm ahead of the spray atomization zone) and Charge carrying distances (50 cm, 100 cm, 150 cm, 200 cm and 250 cm coaxially from the nozzle tip) were the independent variables, whereas the CMR (Charge to Mass Ratio) with three replications was taken as the dependent variable for the statistical analysis. All the statistical procedures were conducted using computer based data analysis software SPSS (Ver. 2016), IBM Inc.

3.14 Cost Economics

The cost effectiveness of the developed system could be estimated in terms of initial cost of the equipment, quantity of chemical used, cost of cultivation and environmental contamination.

CHAPTER IV
RESULTS AND DISCUSSION

In this chapter, the results obtained by the experimental analysis of developed prototype electrostatic induction charging system as an attachment to the powered knapsack mist blower are detailed analyses and discussed.

4.1 Development of electrostatic induction spray charging system as an attachment to the knapsack power mist blower

Five models of electrostatic charge induction systems (Model I, Model II, Model III, Model IV and Model V) were developed during the study in a sequence as an attachment to the powered knapsack mist blower. On evaluation, the first two models (Model I and Model II) did not induce charge to the spray particles. Hence, the other three models (Model III, Model IV and Model V) were developed. The modification of each model was done after its evaluation; hence it was a sequential developmental procedure towards the Model V from Model I.

The models (Model III, Model IV and Model V) were evaluated for Charge to Mass Ratio (CMR) under specific range of charging voltages (1 kV, 2 kV, 3 kV, 4 kV and 5 kV), Electrode placement positions (0 mm, 5 mm, 10 mm and 15 mm ahead of the spray atomization zone) with respect to charge carrying distances (50 cm, 100 cm, 150 cm, 200 cm and 250 cm coaxially from the nozzle tip).

In Model I and II, the charge induction at all the electrode voltage potentials was zero due to the large droplet size (500 µm to 1500 µm) and discharge rate (5 lit. min^{-1}) even at maximum velocity of air in full throttle of engine. The exposed electrode assembly was developed for inducing charge to the droplets and placed 25 mm radial distance from the axis of nozzle. The liquid outlet was disc type with 20 radial oriented emitting orifices of diameter 2 mm.

The discharge rate of nozzle was reduced by modifying the liquid outlet orifice (Model II). The numbers of orifices were reduced from 20 to 6, with diameter 1 mm and the discharge rate was reduced from 5 $lit.min^{-1}$ to 1.5 $lit.min^{-1}$.

However, this model also performed zero voltage induction on droplet produced (500 µm to 1000 µm) under all the electrode voltage potentials.

Hence, a self-atomizing nozzle with external hydraulic power (diaphragm pump working with 12 V DC) was developed. This nozzle could generate a uniform spray droplet spectrum (80 µm to 250 µm) at constant discharge rate (90 ml min^{-1}) and independent of air velocity. This developed self-atomizing hydraulic nozzle was then paired with the exposed electrode assembly (Model III) and evaluated for the five specific electrode voltage potentials (1 kV, 2 kV, 3 kV, 4 kV and 5 kV), four electrode placement positions (EPP 0 mm, EPP 5 mm, EPP 10 mm and EPP 15 mm ahead of the atomization) and five specific charge carrying distances away from the nozzle tip.

The Model III was able to induce charge onto the droplets formed by developed self-atomizing hydraulic nozzle. The maximum CMR value (0.888 $mC.kg^{-1}$) for EPP 5 mm and 5 kV electrode potential voltage at 50 cm distance away from the nozzle tip was observed. Though this model was capable of inducing good charge on droplets, the problems of voltage drop due to electrode wetting and possibilities of corrosion of electrode due to action of agricultural chemicals as well as human life hazards due to direct contact with the electrode were observed, since the HVDC charging electrode was exposed.

To overcome the mentioned drawbacks, a new electrode carrier assembly with embedded electrode was designed and fabricated. This embedded electrode carrier design eliminated all the hurdles related to voltage drop, corrosion and human casualties, as the high voltage electrode was fully insulated within the casing assembly. The combination of self-atomizing nozzle with developed embedded electrode casing assembly (Model IV) was evaluated for the five specific electrode voltage potentials (1 kV, 2 kV, 3 kV, 4 kV and 5 kV), four electrode placement positions (EPP 0 mm, EPP 5 mm, EPP 10 mm and EPP 15 mm ahead of the atomization) and five specific charge carrying distances away from the nozzle tip. The Model IV also could able to induce charge to the droplets formed by developed self-atomizing hydraulic nozzle and shown the maximum

CMR value (0.777 mC.kg^{-1}) for EPP 5 mm and 5 kV electrode potential voltage at 50 cm distance away from the nozzle tip. A slight reduction was observed in charge induction due to insulator interference.

An attempt was made to enhance the droplet chargeability by modifying the embedded electrode carrier assembly. The radial placement of charging ring electrode was reduced from 25 mm to 15 mm from the nozzle axis, in order to bring the HVDC charging electrode closer to the spray atomization zone. As the charging electrode was brought near to the atomization zone, electric field intensity across the droplet formation zone became higher, hence it resulted high rate of charge induction on spray droplets than the Model III and Model IV.

The combination of self-atomizing nozzle with the modified embedded electrode carrier assembly (Model V) was evaluated for the combination of five specific electrode voltage potentials, four electrode placement positions and five specific charge carrying distances away from the nozzle tip. A significant increase was observed in charge induction on spray droplet as the Model V with maximum CMR value of 1.088 mC.kg^{-1}, for 5 kV electrode potential and EPP 5 mm at 50 cm distance away from the spray nozzle coaxially. The CMR values obtained for the Model V were significantly higher than the other two models (Model III and Model IV) at all combinations of the specified variables.

4.2 Measurement of Charge to Mass Ratio

4.2.1 Charge carrying capacity for Model III : Exposed electrode

The CMR of exposed electrode electrostatic induction charging model (Model III) has shown the highest value of (0.888 mC.kg^{-1}) at charging voltage potential of 5 kV for electrode placement positions II (5 mm) at charge carrying distance of 50 cm. The CMR values were observed gradually increasing (from 0.067 to 0.888 mC.kg^{-1}) with increasing electrode potential (from 1 kV to 5 kV) and decreasing with increasing charge carrying distance (Appendix I). There was a slight (5% to 10%) reduction in the overall charge induction with the electrode placement position other than 5 mm ahead of spray atomization.

4.2.2 Charge carrying capacity for Model IV : Embedded electrode

The highest value of CMR for embedded electrode electrostatic induction charging model (Model IV) was observed (0.777 $mC.kg^{-1}$) at charging voltage potential of 5 kV for electrode placement position II (5 mm) at charge carrying distance of 50 cm. The CMR values were observed gradually increasing (from 0.133 to 0.755 $mC.kg^{-1}$) with increasing electrode potential (from 1 kV to 5 kV) and decreasing with increasing charge carrying distance (Appendix II). There was a slight (5% to 10%) reduction observed in the overall charge induction with the electrode placement positions (EPP) other than 5 mm ahead of spray atomization.

The problem of voltage drop due to electrode wetting and corrosion of electrode due to exposure of electrode towards chemicals and health hazards of operator due to direct contact with electrode were completely eliminated by the embedded electrode position.

4.2.3 Charge carrying capacity for Model V : Narrow embedded electrode

The narrow embedded electrode electrostatic induction charging model (Model V) has been shown highest value of CMR (1.088 $mC.kg^{-1}$) over other two models at charging voltage potential of 5 kV for electrode placement-II (5 mm) at charge carrying distance of 50 cm. The CMR values were observed gradually increasing (from 0.422 to 1.088 $mC.kg^{-1}$) with increasing electrode potential (from 1 kV to 5 kV) and decreasing with increasing charge carrying distance (Appendix III). There was a slight (5% to 10%) reduction observed in the overall charge induction with the electrode placements other than 5 mm ahead of spray atomization.

The narrow embedded electrode (Model V) charging system has shown the highest electrostatic charge induction on the spray droplets over Model III and Model IV, in all combinations of variables and in respect of the charge carrying capacity. The higher air velocity (110 to 120 $m.s^{-1}$) resulted from the narrow orifice protected the wetting of electrode assembly and gave air assistance to the spray droplets to the longer distance.

4.3 Effect of electrode voltage potential on charge induction (CMR)

The CMR of the charged droplets at different electrode voltage potentials (1 kV, 2 kV, 3 kV, 4 kV and 5 kV), Electrode placement position (0 mm, 5 mm, 10 mm and 15 mm ahead of the spray atomization) and at five different distances from the nozzle tip were evaluated for all the three models (Model III, Model IV and Model V). The maximum CMR value (1.088 $mC.kg^{-1}$) was observed for Model V at 50 cm distance from the nozzle and 5 mm electrode placement position with 5 kV electrode voltage potential, followed by Model III (0.888 $mC.kg^{-1}$) and Model IV (0.777 $mC.kg^{-1}$) at 5 mm electrode placement position and 5 kV electrode potential at 50 cm distance from nozzle tip. For each model the CMR was observed maximum for 5 kV electrode voltage potential and 5 mm electrode placement position at 50 cm distance away from the spray nozzle and reduced gradually with decrease in electrode voltage potential.

The CMR measured at 50 cm coaxially ahead of the spray nozzle at five specific voltages (1 kV, 2 kV, 3 kV, 4 kV and 5 kV) and elctrode placement positions (EPP 0 mm, EPP 5 mm, EPP 10 mm and EPP 15 mm) ahead of the atomization zone for all the three developed models (Model III, Model IV and Model V) are represented in Fig. 16 to Fig. 35. It was evident that Model V with electrode voltage potential at 5 kV and EPP at 5 mm shown the maximum CMR value (1.088 $mC.kg^{-1}$), followed by Model III (0.888 $mC.kg^{-1}$) and Model IV (0.775 mC.kg-1) with same combination of variables.

Among the three models, the CMR values at all electrode voltage potentials were significantly higher for Model V than the other two. This trend could be justified with the high electrostatic field intensity that produced due to high voltage and low gap between the positive charging electrode and atomization zone, resulted in higher the charge induction on droplets.

4.4 Effect of electrode placement position on charge induction (CMR)

For all models, the charge induction was maximum for EPP 5 mm ahead of the spray atomization zone (Fig. 16 to Fig. 35). This result could be justified by the atomization lag of the nozzle i.e. just after the nozzle orifice, the water

performed like a sheet immediately before the atomization. This lag restricted the formation of the droplet and hence the charge induction in case of EPP 0 mm. Whereas in case of EPP 10 mm and EPP 15 mm, the droplets formed at the atomization zone were rapidly carried away by the high velocity air stream, resulted reduction of exposure time of droplets towards electrostatic field, and caused a slight reduction in the charge induction on the droplets.

The CMR of charged droplets at different electrode placement positions (0 mm, 5 mm, 10 mm and 15 mm ahead of the spray atomization) and at five different distances from the nozzle tip were evaluated for all the three models (Model III, Model IV and Model V) and the results of Multiple Comparison Test were as detailed in Appendix IV. For each model the CMR was observed maximum for 5 kV electrode voltage potential and 5 mm electrode placement position, at 50 cm distance away from the spray nozzle as compared with EPP 0 mm, EPP 10 mm and EPP 15 mm.

For each model (Model III, Model IV and Model V) with all stages of electrode voltage potential, CMR was increased from EPP 0 mm to EPP 5 mm gradually and started reducing thereafter for EPP 10 mm onwards followed by EPP 15 mm.

4.5 Effect of Charge carrying distance on CMR

For all the three models (Model III, Model IV and Model V) the charge carrying capacity was maximum at electrode voltage potential of 5 kV with the electrode placement position at 5 mm ahead of atomization zone, for all the five coaxial measuring distances from the spray nozzle tip (50 cm, 100 cm, 150 cm, 200 cm and 250 cm). The maximum charge carrying capacity was observed for Model V (1.088 $mC.kg^{-1}$ to 0.111 $mC.kg^{-1}$) followed by Model III (0.888 $mC.kg^{-1}$ to 0.067 $mC.kg^{-1}$) and Model IV (0.777 $mC.kg^{-1}$to 0.056 $mC.kg^{-1}$) in ascending distance order (Fig. 36). The CMR values were observed reducing with the increase in distance of measurement from the nozzle for all three models. The reduction in CMR could be due to the higher rate of diffusion of spray jet at longer distances from atomization zone.

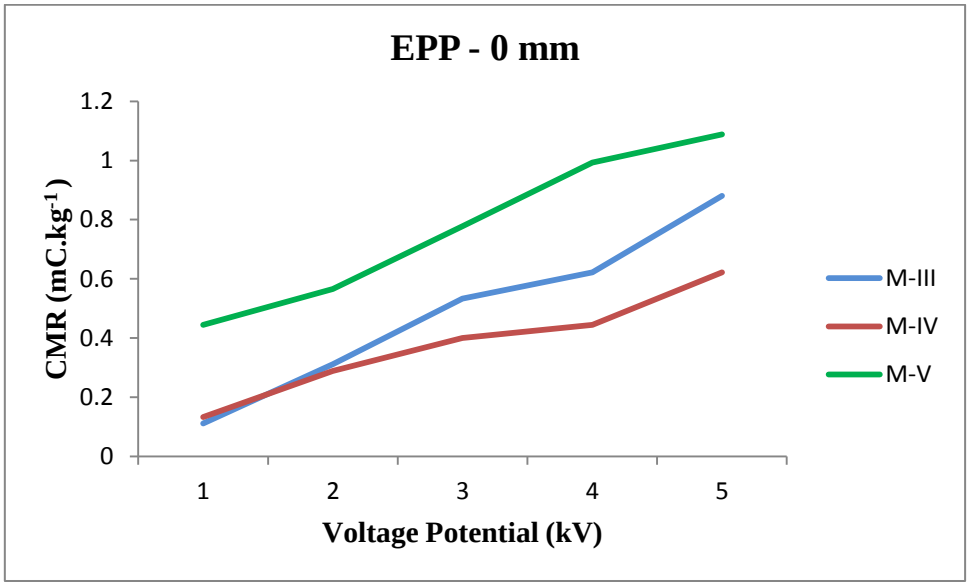

Fig. 16 Effect of electrode voltage potential on charge induction (CMR) at 50 cm ahead of nozzle and EPP - 0 mm

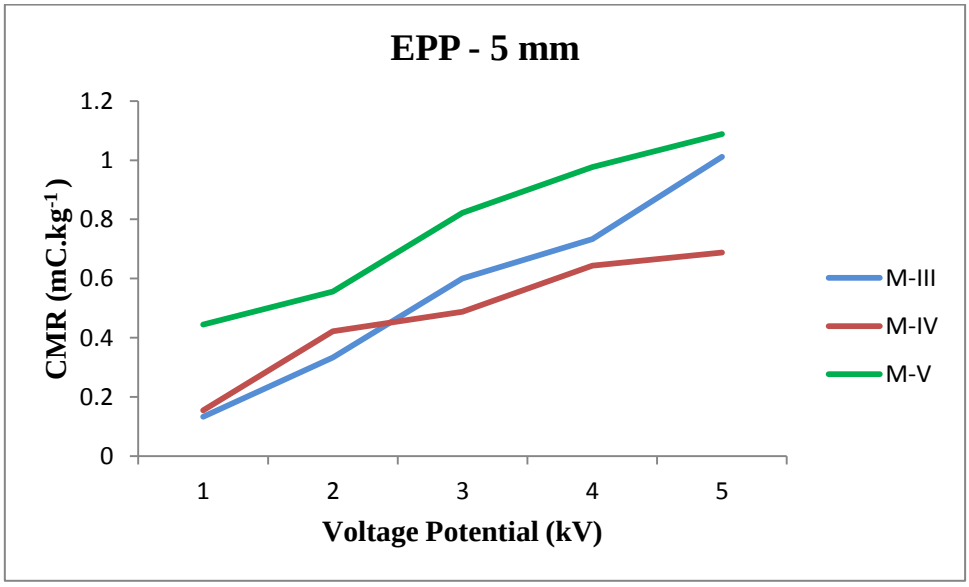

Fig. 17 Effect of electrode voltage potential on charge induction (CMR) at 50 cm ahead of nozzle and EPP - 5 mm

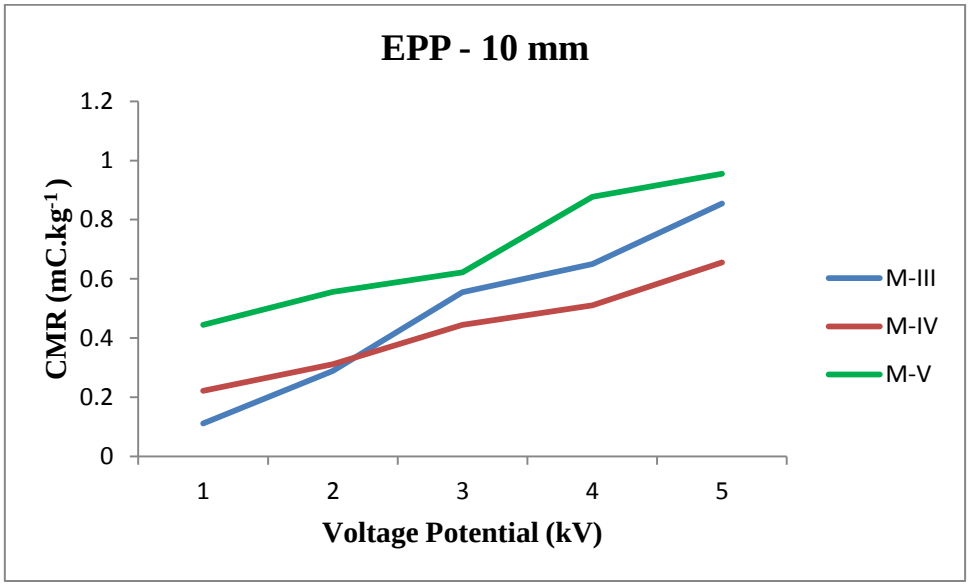

Fig. 18 Effect of electrode voltage potential on charge induction (CMR) at 50 cm ahead of nozzle and EPP - 10 mm

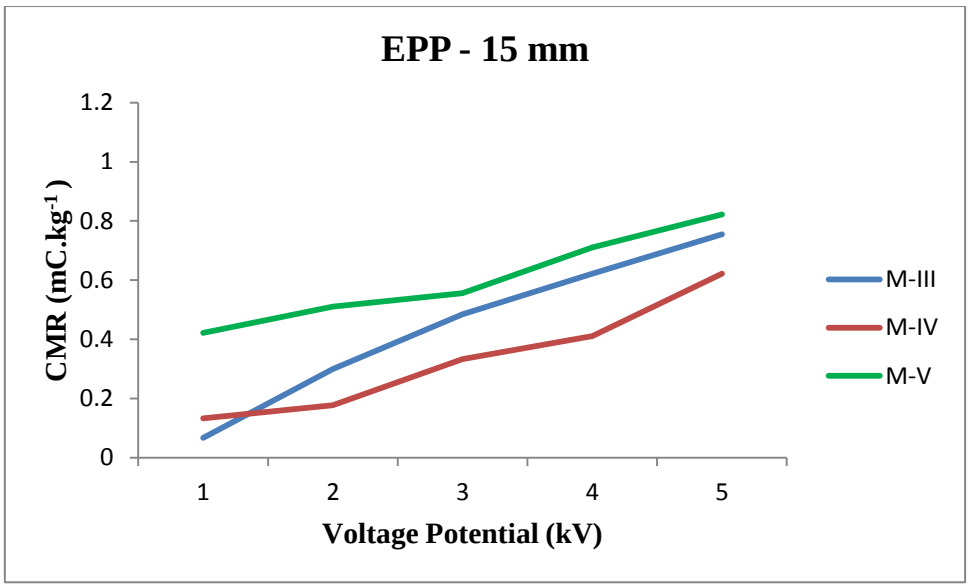

Fig. 19 Effect of electrode voltage potential on charge induction (CMR) at 50 cm ahead of nozzle and EPP - 15 mm

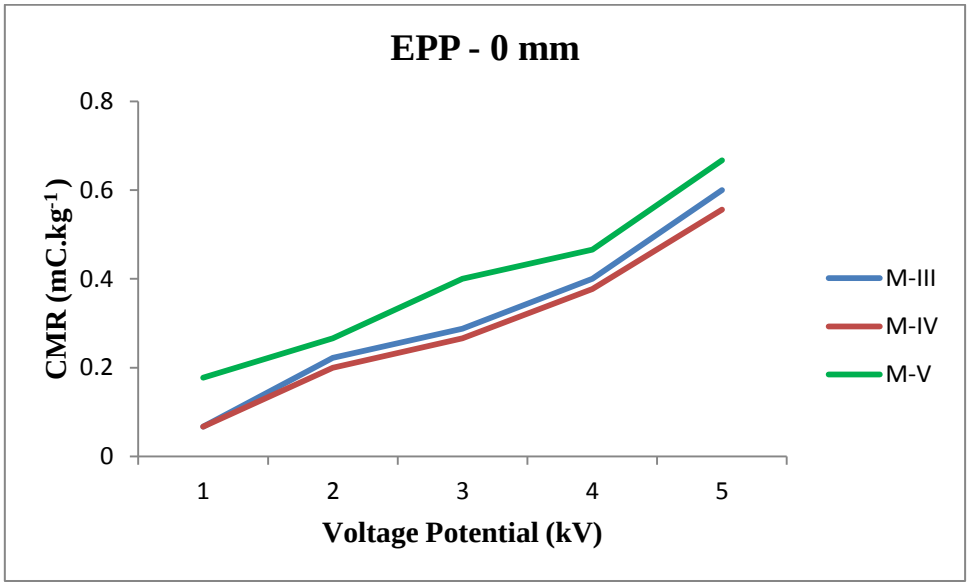

Fig. 20 Effect of electrode voltage potential on charge induction (CMR) at 100 cm ahead of nozzle and EPP - 0 mm

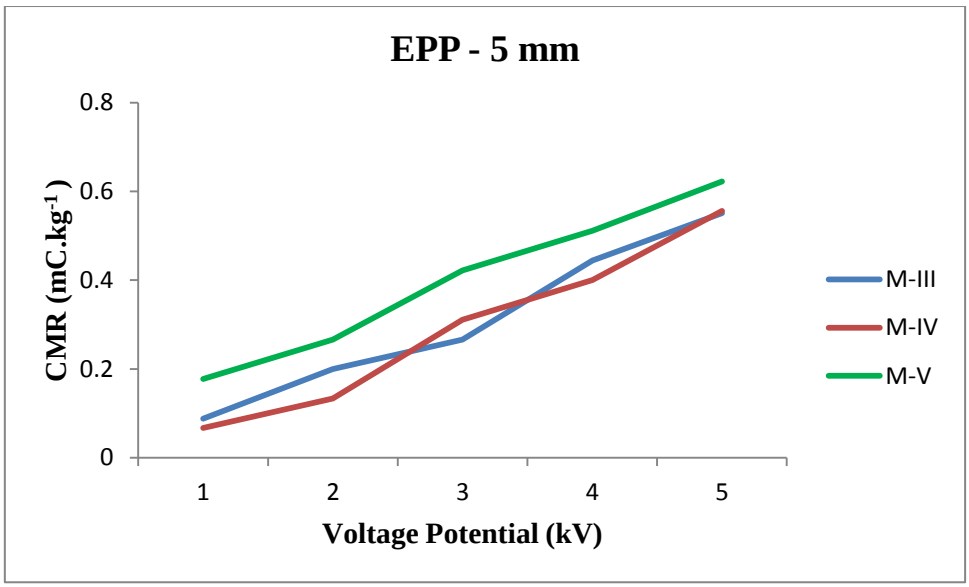

Fig. 21 Effect of electrode voltage potential on charge induction (CMR) at 100 cm ahead of nozzle and EPP - 5 mm

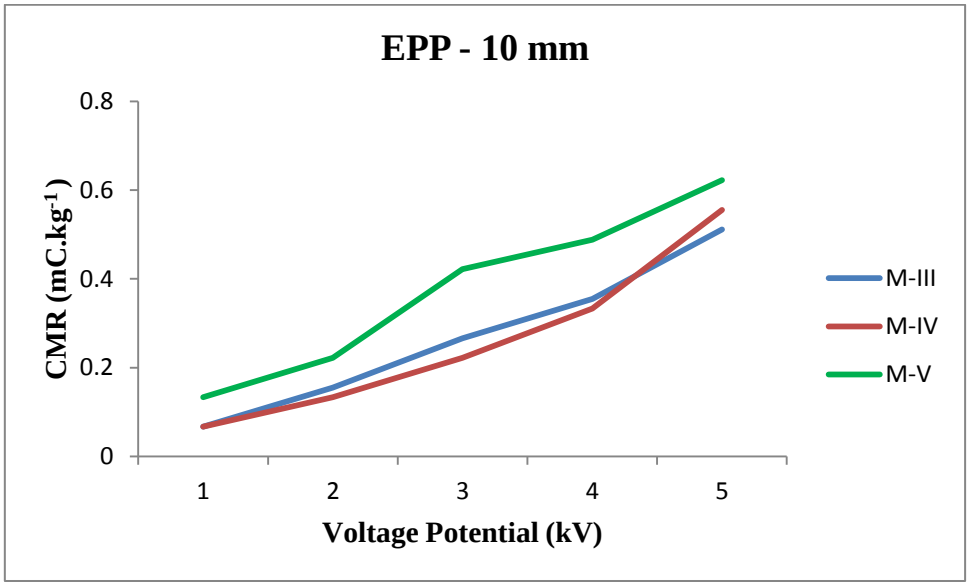

Fig. 22 Effect of electrode voltage potential on charge induction (CMR) at 100 cm ahead of nozzle and EPP - 10 mm

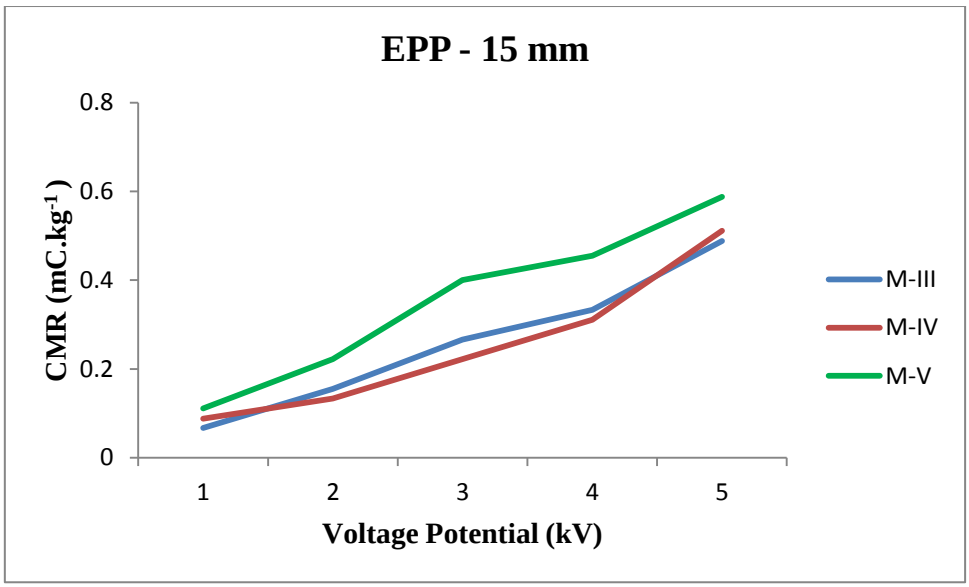

Fig. 23 Effect of electrode voltage potential on charge induction (CMR) at 100 cm ahead of nozzle and EPP - 15 mm

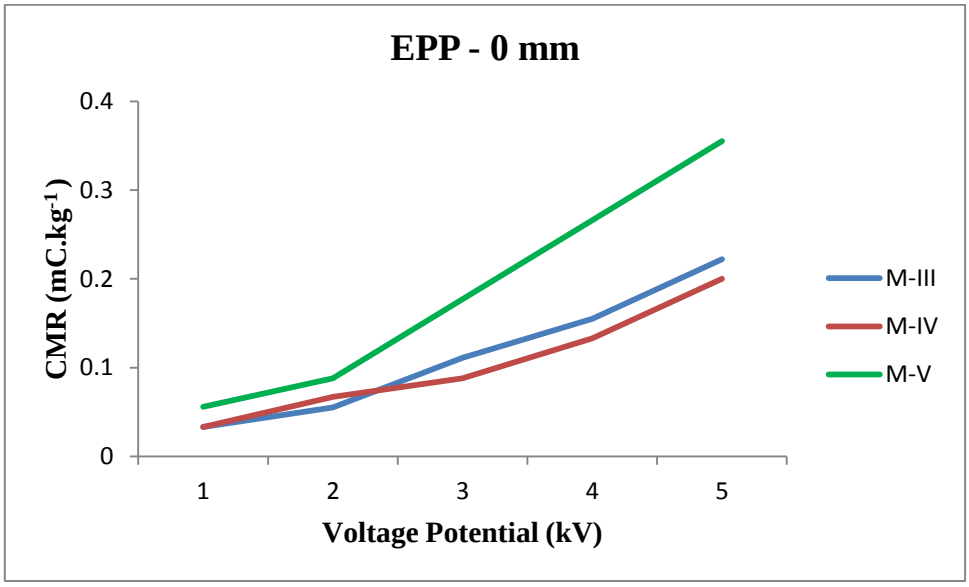

Fig. 24 Effect of electrode voltage potential on charge induction (CMR) at 150 cm ahead of nozzle and EPP - 0 mm

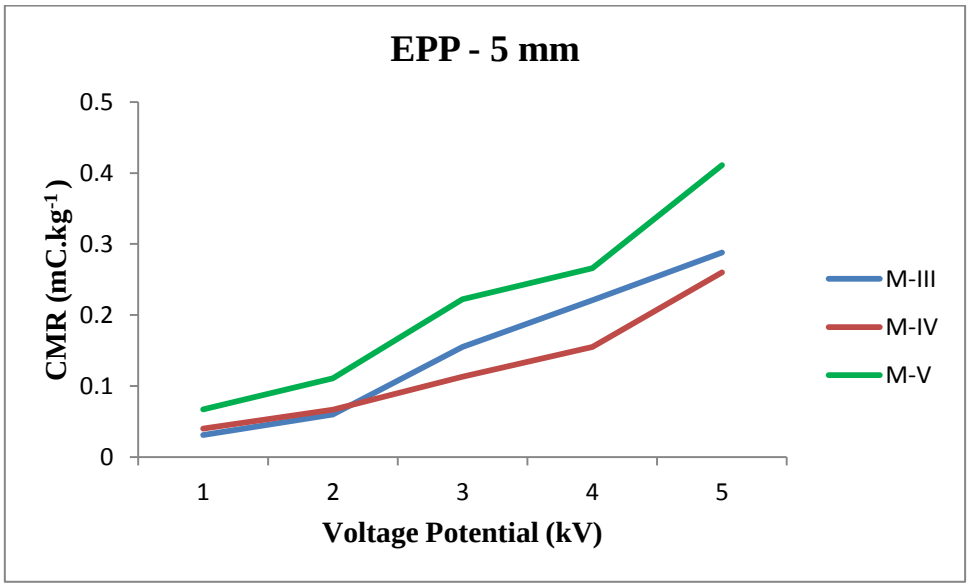

Fig. 25 Effect of electrode voltage potential on charge induction (CMR) at 150 cm ahead of nozzle and EPP - 5 mm

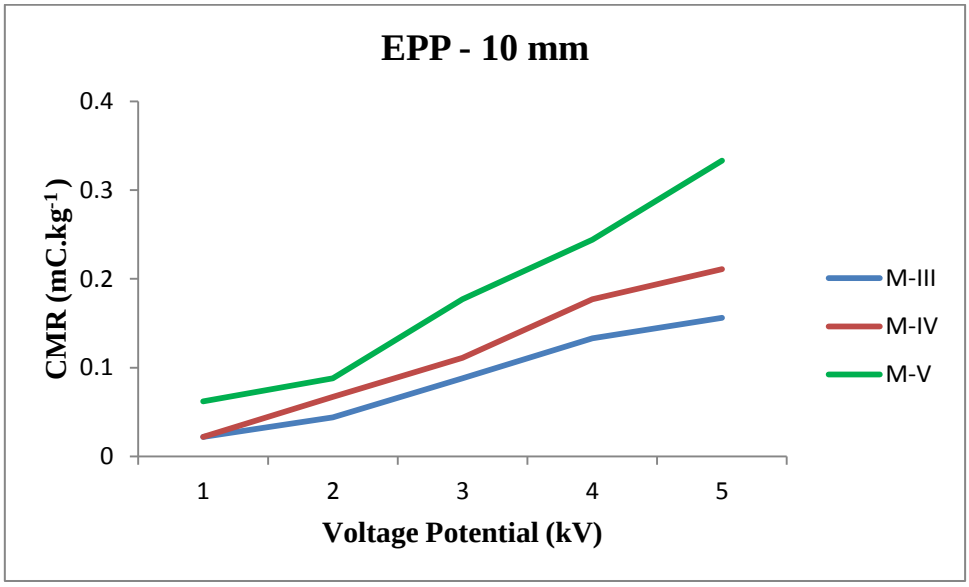

Fig. 26 Effect of electrode voltage potential on charge induction (CMR) at 150 cm ahead of nozzle and EPP - 10 mm

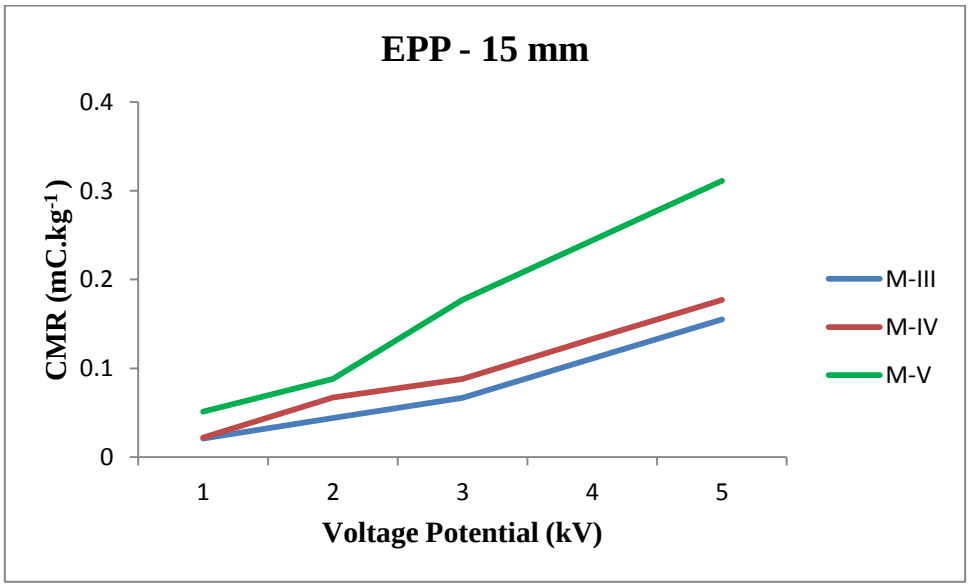

Fig. 27 Effect of electrode voltage potential on charge induction (CMR) at 150 cm ahead of nozzle and EPP - 15 mm

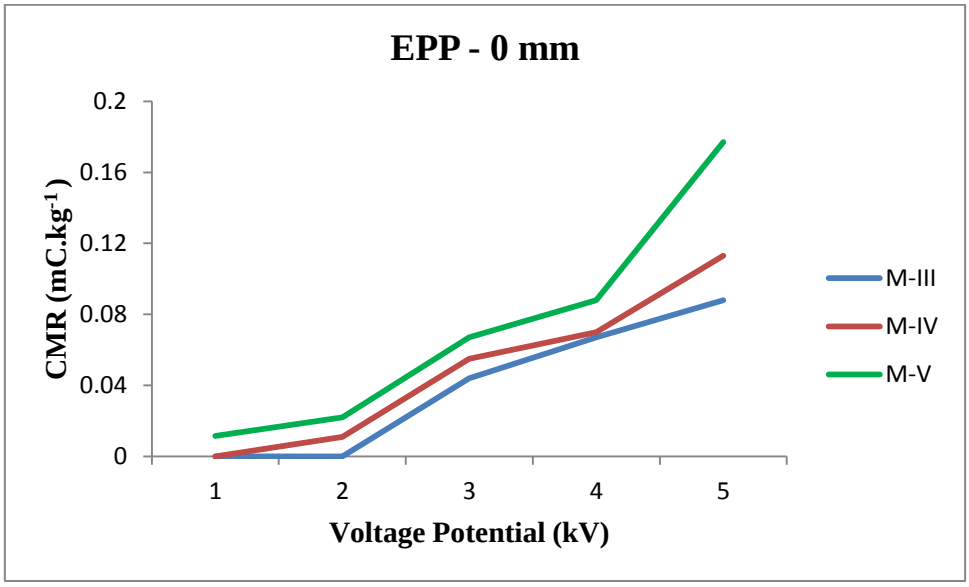

Fig. 28 Effect of electrode voltage potential on charge induction (CMR) at 200 cm ahead of nozzle and EPP - 0 mm

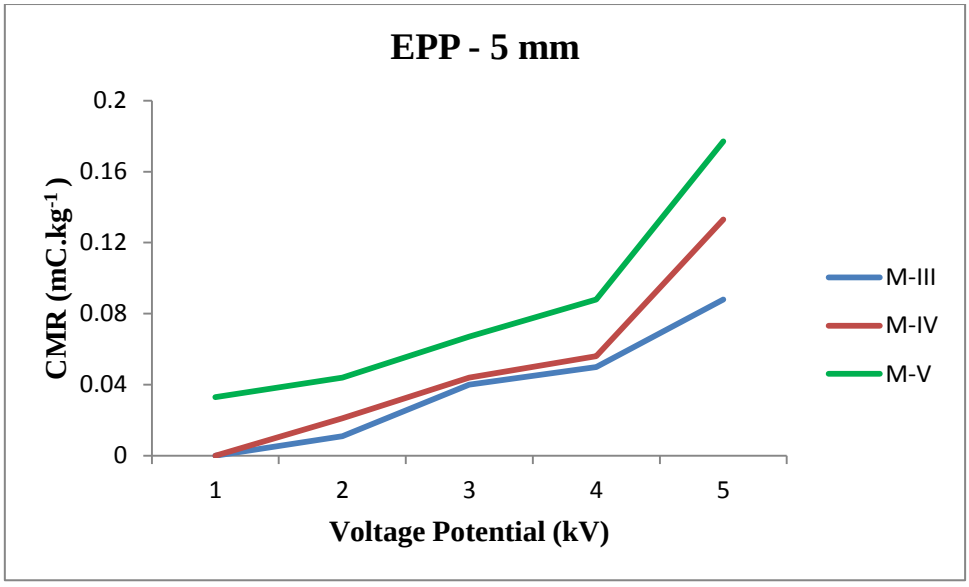

Fig. 29 Effect of electrode voltage potential on charge induction (CMR) at 200 cm ahead of nozzle and EPP - 5 mm

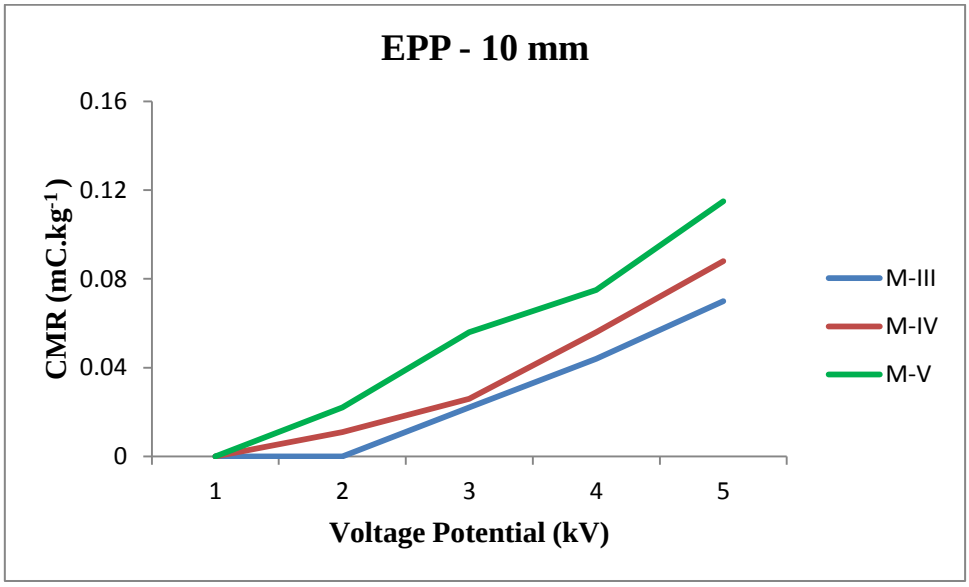

Fig. 30 Effect of electrode voltage potential on charge induction (CMR) at 200 cm ahead of nozzle and EPP - 10 mm

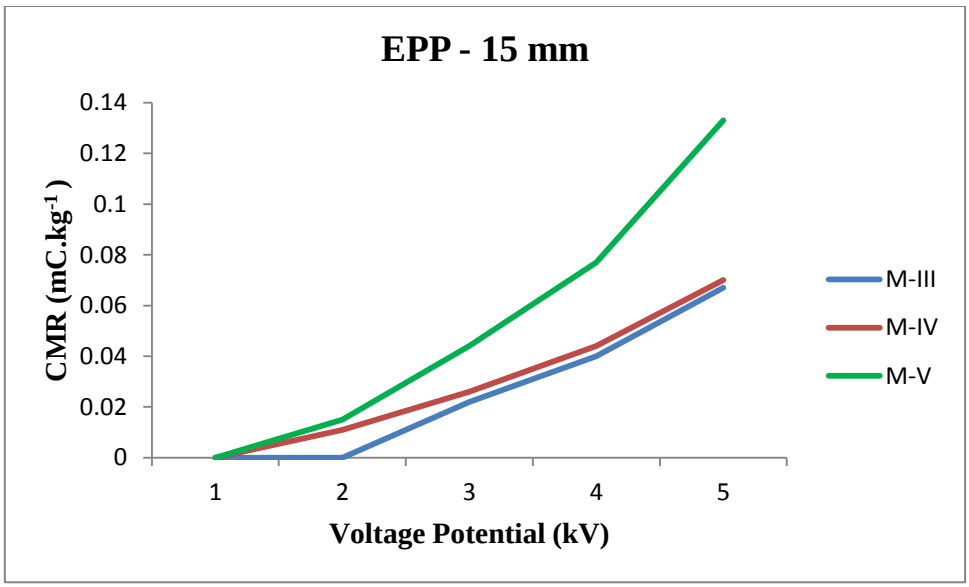

Fig. 31 Effect of electrode voltage potential on charge induction (CMR) at 200 cm ahead of nozzle and EPP - 15 mm

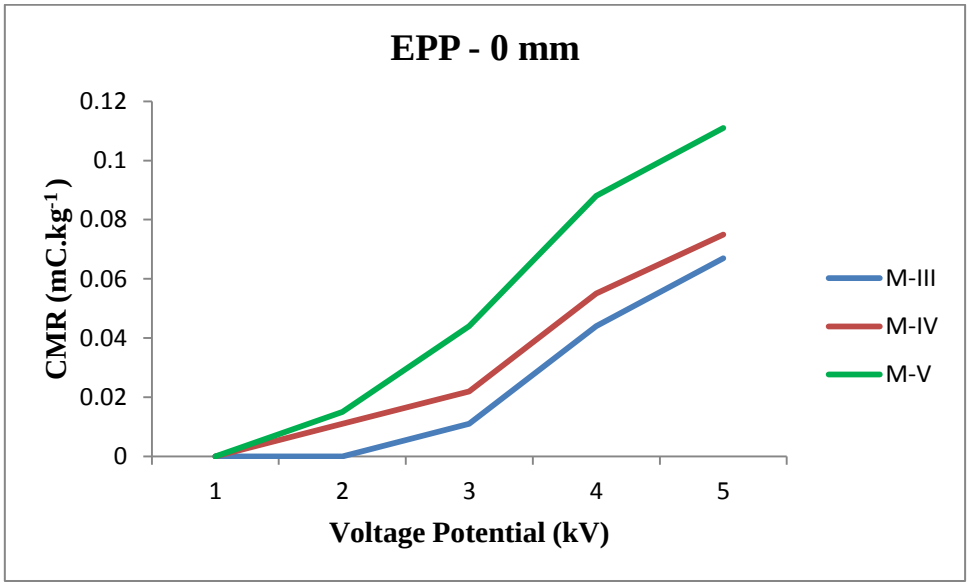

Fig. 32 Effect of electrode voltage potential on charge induction (CMR) at 250 cm ahead of nozzle and EPP - 0 mm

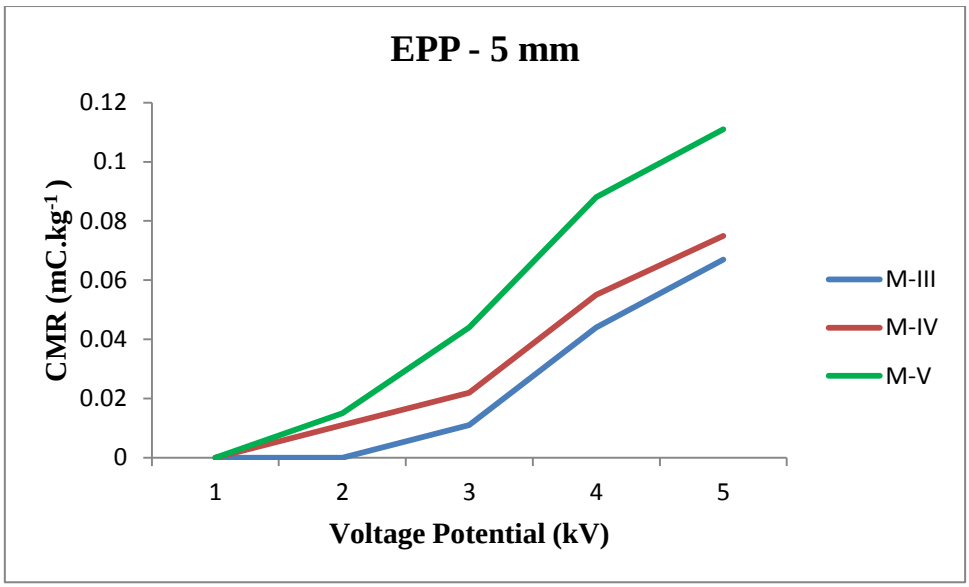

Fig. 33 Effect of electrode voltage potential on charge induction (CMR) at 250 cm ahead of nozzle and EPP - 5 mm

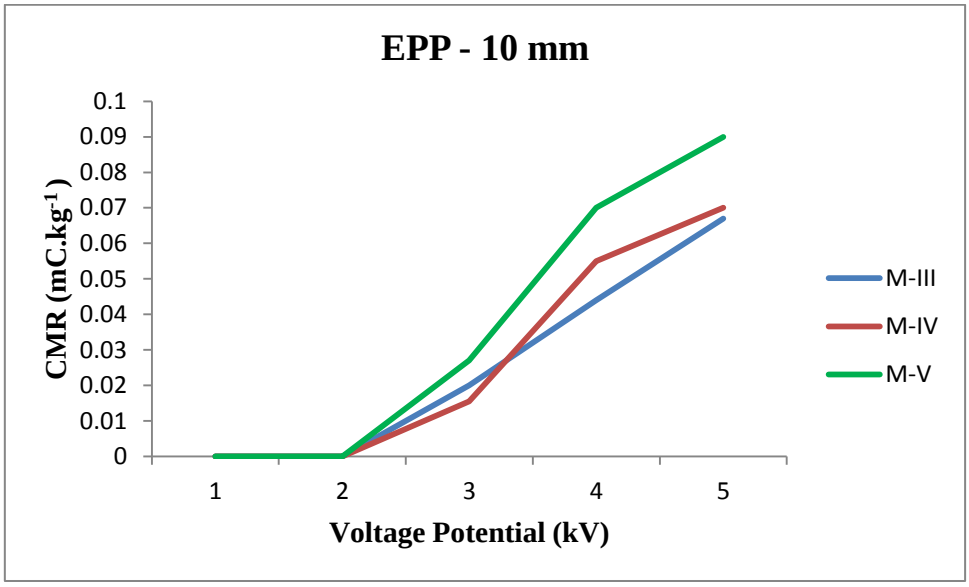

Fig. 34 Effect of electrode voltage potential on charge induction (CMR) at 250 cm ahead of nozzle and EPP - 10 mm

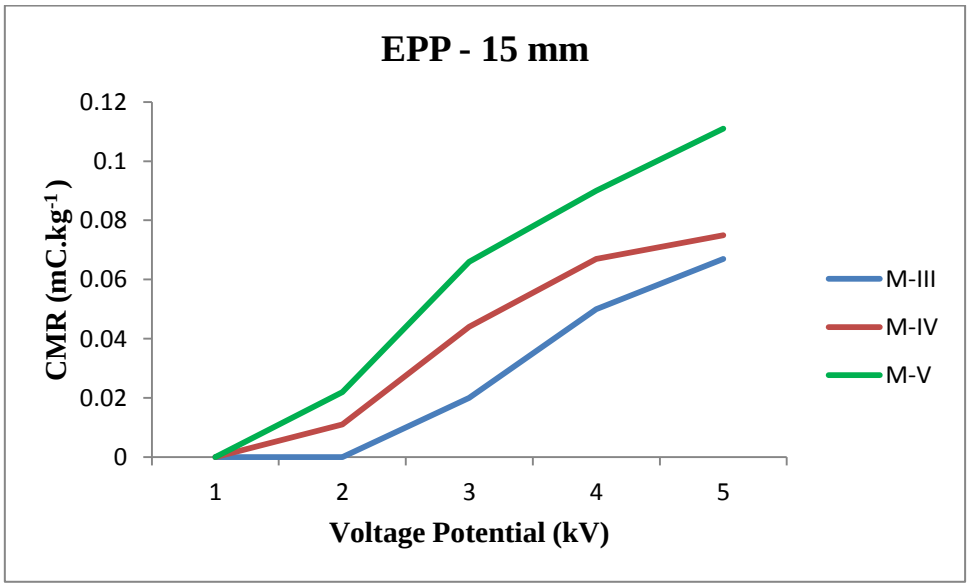

Fig. 35 Effect of electrode voltage potential on charge induction (CMR) at 250 cm ahead of nozzle and EPP - 15 mm

4.6 Analysis of variance (ANOVA)

The acquaint data were processed and analyzed for variance with Single Factor One-Way ANOVA. For five variable charging potentials (1 kV to 5 kV) and five charge carrying distances (50 cm to 250 cm) separate ANOVA were followed for better analysis between the groups at 95 percent confidence level. The single factor one-way ANOVA has showed that Model V was overall significant in all the experimental setups. The different ANOVAs done were as mentioned in Table 1.

Table 1. Effect of electrode potential on CMR

Model III, IV & V	**Charging electrode potential**				
Statistical parameter	**1 kV**	**2 kV**	**3 kV**	**4 kV**	**5 kV**
At 50 cm away from nozzle					
F	160.412	21.205	8.945	5.853	19.255
P	9.1E-08	0.0004	0.0073	0.0235	0.00056
$F_{critical}$	4.256	4.256	4.256	4.256	4.256
Significance (α = 0.05)	**S**	**S**	**S**	**S**	**S**
At 100 cm away from nozzle					
F	18.245	5.357	44.932	1.0156	2.340
P	0.000681	0.0293	2.07E-05	0.400	0.152
$F_{critical}$	4.256	4.256	4.256	4.256	4.256
Significance (α = 0.05)	**S**	**S**	**S**	**NS**	**NS**
At 150 cm away from nozzle					
F	30.095	21.901	0.946	10.289	7.397

P	0.000103	0.000348	0.42322	0.00472	0.01258
$F_{critical}$	4.256	4.256	4.256	4.256	4.256
Significance (α = 0.05)	**S**	**S**	**NS**	**S**	**S**

At 200 cm away from nozzle					
F	2.777	5.888	4.241	5.954	14.647
P	0.11493	0.02332	0.05039	0.02252	0.00148
$F_{critical}$	4.256	4.256	4.256	4.256	4.256
Significance (α = 0.05)	**NS**	**S**	**NS**	**S**	**S**
At 250 cm away from nozzle					
F	65535	3	3.822	16	21.157
P	0	0.10038	0.06284	0.00093	0.000396
$F_{critical}$	4.256	4.256	4.256	4.256	4.256
Significance (α = 0.05)	**S**	**NS**	**NS**	**S**	**S**

4.7 Measurement of spray droplet size

The spray droplet size was measured for the developed self-atomizing hydraulic nozzle using bromide photo papers with pigmented spray solution and IMAGE-J image analyzing computer software. The observed spray droplet size measured at constant nozzle operating pressure (2.5 $kg.cm^{-2}$) and at 1.0 m, 1.5 m and 2.0 m horizontal distance was in the range of 80 µm to 250 µm, which was

found to be in the required spectrum of effective electrostatic induction chargeability of the spray. The reduced droplet size from the developed hydraulic nozzle enhanced deposition characters also.

The droplet spectrum was one of the major constraints while dealing with the development of electrostatic charge induction system to induce charge on the spray droplets. Since, the droplet diameter (500 µm to 1500 µm) of the existing nozzle was of much higher than the required one (40 µm to 300 µm), Model I failed to produce charge induction at all the electrode voltage potential even at full engine throttle with maximum air velocity. For reducing the droplet size a modified nozzle (Model II) was fabricated with reduced discharging orifices. But the Model II also failed to induce charge under all electrode voltage potential, since the droplet size (500 µm to 1000 µm) was still beyond the desired range.

A self-atomizing hydraulic pressure nozzle was hypothesized and developed accordingly. This nozzle was operated by a LDHP 12V dc diaphragm pump and could generate a fine spray droplet diameter (80 µm to 250 µm) at constant discharge rate (90 ml min^{-1}) and independent of blower air velocity. The droplet size analysis was performed with bromide photo paper method and IMAGE-J image analyzing computer software.

4.8 Deposition characteristics

The performance evaluation of the developed models was done by quantifying the deposition efficiency within the models and versus uncharged spray as explained in Table 2. The spray application was done on Pepper vines having smooth leaf and dense canopy (Plate 10.). The spray was applied towards the plant by keeping the nozzle 100 cm to 150 cm away from the plant to avoid injury due high velocity air blow, at maximum charge induction potential. The electrostatically charged sprays (Model III, IV and V) achieved higher deposition efficiency (40 to 70%) than uncharged spray (25 to 40%) on overall plant body Plate 11, Plate 12 and Plate 13). The Model V gave highest deposition efficiency (40 to 70%) than other two models (Model III : 40 to 65%, Model IV : 35 to 60%) and uncharged spray (25 to 40%).

Table 2. Deposition efficiency

Plant Target	Deposition Efficiency, %		
	Electrostatic Spray		Uncharged air-assisted spray
	Commercial ESS unit	Developed Model V	
Leaf Top Surface	65 to 70	60 to 70	30 to 40
Leaf Bottom	55 to 65	50 to 60	25 to 30
Plant Body – Stem	45 to 55	40 to 50	25 to 30

4.9 Comparison with commercial electrostatic sprayer

The developed electrostatic spray charging system (Model V) was evaluated for CMR in comparison with existing commercial electrostatic sprayer of make Electrostatic Spraying Systems (ESS) Inc., Watkinsville (G.A.) Model-ESS-MBP90. The CMR values were measured for both developed and existing ESS sprayer at different distances (50 cm, 100 cm, 150 cm, 200 cm and 250 cm) coaxially from the spray nozzle tip and expressed in Table 3.

Table 3. CMR comparison between commercial and developed system

Sprayer Model	CMR ($mC.kg^{-1}$) at distances from the nozzle				
	50 cm	100 cm	150 cm	200 cm	250 cm
Commercial ESS	2.121	0.561	0.221	0.044	0.022
Developed Model V	1.088	0.677	0.444	0.177	0.111

The maximum CMR (2.12 $mC.kg^{-1}$) was observed at 50 cm distance away from nozzle for commercial electrostatic sprayer (ESS-MBP90), followed by developed unit (1.088 $mC.kg^{-1}$) at optimum operating conditions. The observed CMR values were ranged between 0.022 $mC.kg^{-1}$to 2.121 $mC.kg^{-1}$ and 0.111

$mC.kg^{-1}$ to 1.088 $mC.kg^{-1}$ for commercial ESS sprayer and developed Model-V respectively in descending distance from the spray nozzle.

The commercial electrostatic sprayer utilizes high pressure compressed air to atomize the spray liquid with discharged rate of 150 $ml.min^{-1}$. On the other hand the developed self-atomizing nozzle atomizes the spray liquid by virtue of hydraulic pressure through portable 12V DC diaphragm pump and was independent of air velocity. Hence the air stream from mist blower was utilized only for directing the charged spray droplets towards the target. The CMR values were measured for both developed system (for 1 kV to 5 kV and EPP 5 mm) and existing ESS sprayer at different distances (50 cm, 100 cm, 150 cm, 200 cm and 250 cm) coaxially from the spray nozzle tip.

The maximum CMR (2.12 $mC.kg^{-1}$) was observed at 50 cm distance away from nozzle for commercial electrostatic sprayer (ESS-MBP90), followed by prototype (1.088 $mC.kg^{-1}$) at optimum operating conditions (Fig. 37). The observed CMR values were ranged between 0.022 $mC.kg^{-1}$to 2.121 $mC.kg^{-1}$ and 0.111 $mC.kg^{-1}$ to 1.088 $mC.kg^{-1}$ for commercial ESS sprayer and developed Model-V respectively from 250 cm to 50 cm distance from the spray nozzle.

Plate 10. Spray Deposition on upper leaf surface - Electrostatic Sprayer

Plate 11. Spray Deposition on under leaf surface - Electrostatic Sprayer

Plate 12. Spray Deposition on Pepper leaf surface –
Uncharged Air-assisted Spray

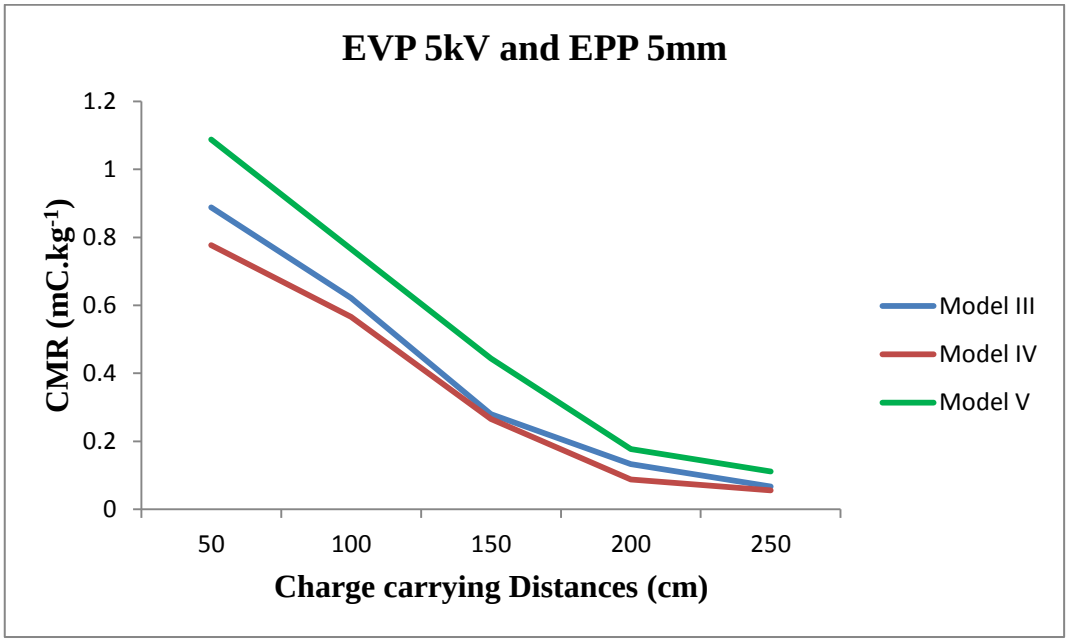

Fig. 36 Effect of Charge carrying distance on CMR

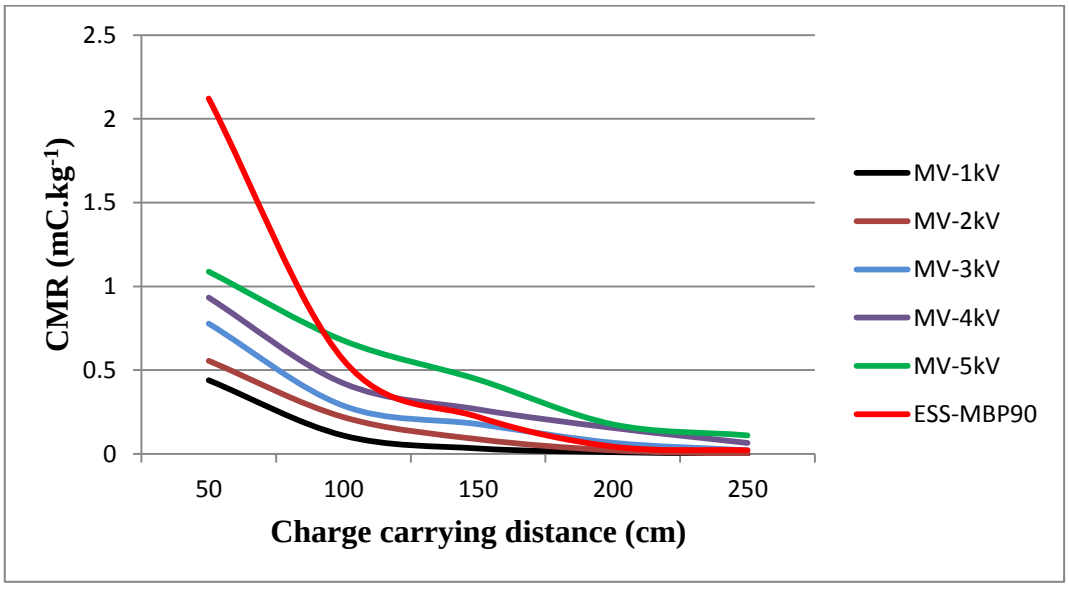

Fig. 37 Charge carrying capacity: Developed system (Model V) with five charging voltages Vs. Commercial ESS-MBP90 sprayer

It was observed that the developed electrostatic induction charging system surpassed the commercial ESS unit for CMR from 100 cm onwards, as the CMR

value for commercial unit radically lowered from 2.12 $mC.kg^{-1}$ to 0.561 $mC.kg^{-1}$ within first 50 cm increment (from 50 cm to 100 cm) in charge carrying distance. However, the developed system shown significantly low rate of CMR reduction (1.088 $mC.kg^{-1}$ to 0.111 $mC.kg^{-1}$) in respect of travel distances which in turn reflected its better charge carrying capacity than the commercial unit (2.121 $mC.kg^{-1}$ to 0.022 $mC.kg^{-1}$).

4.10 Cost Economics

The cost effectiveness of the developed system was estimated in terms of initial cost of the equipment, quantity of chemical used, cost of cultivation and environmental contamination.

Table 4. Cost Economics of the developed system

Particulars	Air-assisted spray system	Commercial Electrostatic spray system	Developed Electrostatic spray system
Deposition efficiency	30 to 40 %	65 to 70 %	60 to 70 %
Chemical used	More than 4 times the recommended dosage	Less than 1.5 times the recommended dosage	Less than 1.5 times the recommended dosage
Reduction in cost of cultivation	5 to 10 %	25 to 35 %	25 to 35 %
Environmental contamination	75 to 80 %	20 to 35 %	20 to 25 %
Initial Cost (Approx.)	Rs. 50,000/-	Rs. 400,000/-	Rs. 65,000/- (Including sprayer)

CHAPTER V

SUMMARY AND CONCLUSIONS

The introduction of electrically charged sprays in agricultural application has become inescapable for superior control on droplet transference with reduced drift and increased application efficiency with less spray chemical expenditure. The development of an economical electrostatic spray charging system as an attachment to the popular knapsack mist blower will be a boon to the Indian farmer. Hence, the study was contemplated at Department of Agricultural Engineering, College of Agriculture, Vellayani, Kerala Agricultural University during 2015 to 2016.

The objectives of the study were, to develop a low cost electrostatic nozzle and charging system compatible to a DC power source, study the dynamic charge acquisition, spray chargeability and depositional characteristics of the charged spray on plant targets of the developed system.

Experimental prototype of induction charging nozzle attachment was developed to suit a knapsack mist blower (OleoMac-AM162). The high voltage generator was fabricated on the basis of Cockcroft-Walton voltage multiplier principle, using 6 V DC battery with 0.25 mA current as an input source. Five different prototypes (Model I to Model V) including the self-atomizing hydraulic nozzle were developed and analysed for the charge induction on spray droplet, out of which only Models III, IV and V were capable of producing effective charge induction on spray droplets.

In Model I and II, the charge induction at all the five electrode voltage potentials (1 kV, 2 kV, 3 kV, 4 kV and 5 kV) was zero due to the large droplet size (500 µm to 1500 µm) and discharge rate (1.5 to 5 lit. min^{-1}) even at maximum velocity of air in full throttle of engine. The exposed electrode assembly was developed for inducing charge to the droplets and placed 25 mm radial distance from the axis of nozzle. Hence, self-atomizing nozzle with external hydraulic power was developed. This nozzle could generate fine spray droplets of required diameter (80 µm to 250 µm) at constant discharge rate (90 ml min^{-1}). The nozzle

was then coupled with exposed electrode assembly (Model III), embedded electrode assembly (Model IV) and Narrow embedded electrode assembly (Model V). All the models were evaluated for CMR under specific charging voltages, electrode placement positions (0 mm, 5 mm, 10 mm and 15 mm ahead of the spray atomization zone) with respect to charge carrying distances (50 cm, 100 cm, 150 cm, 200 cm and 250 cm coaxially from the nozzle tip).

- The maximum CMR value (1.088 $mC.kg^{-1}$) was observed for Model V at 50 cm distance from the nozzle and 5 mm electrode placement position with 5 kV electrode voltage potential.
- The second highest CMR (0.888 $mC.kg^{-1}$) was observed for Model III at 5 mm electrode placement position and 5 kV electrode potential at 50 cm distance from nozzle tip.
- Among the three models, the CMR values at all electrode voltage potentials with EPP 5 mm were significantly higher for Model V than the other two.
- This variation in charge induction could be explained with the high electrostatic field intensity that produced due to high voltage and low gap between the positive charging electrode and atomization zone.

The spray droplet size was also measured using bromide photo papers with pigmented spray solution and IMAGE-J image analyzing computer software at constant nozzle operating pressure (2.5 $kg.cm^{-2}$).

- The spray droplet size at 1.0 m, 1.5 m and 2.0 m distance from the nozzle tip was in the range of 80 µm to 250 µm, which was the required spectrum of effective electrostatic induction chargeability of the spray.

The deposition efficiency of the developed system versus uncharged spray was quantified with leaf wash method using fluorescent tracer (DAY GLO type GT-15-N Fluorescent Blaze Orange dye). The leaf samples collected randomly from different parts of target surface (Pepper vines). The dye spray was applied by keeping the nozzle 100 to 150 cm away from the plant to avoid air blast injury.

- The electrostatically charged sprays (Model III, IV and V) achieved higher deposition efficiency (40 to 70%) than uncharged spray (25 to 40%) on overall plant body.

- The Model V gave highest deposition efficiency (40 to 70%) than other two models (Model III : 40 to 65%, Model IV : 35 to 60%) and uncharged spray (25 to 40%).

The developed electrostatic spray charging system (Model V) was evaluated for CMR in comparison with existing commercial electrostatic sprayer of make Electrostatic Spraying Systems (ESS) Inc., Watkinsville (G.A.) Model-ESS-MBP90.

- The maximum CMR (2.12 $mC.kg^{-1}$) was observed at 50 cm distance away from nozzle for commercial electrostatic sprayer (ESS-MBP90), followed by developed unit (1.088 $mC.kg^{-1}$) at optimum operating conditions.
- The CMR were ranged between 0.022 $mC.kg^{-1}$to 2.12 $mC.kg^{-1}$ and 0.111 $mC.kg^{-1}$ to 1.088 $mC.kg^{-1}$ for commercial ESS sprayer and developed Model-V respectively in descending distance from the spray nozzle.
- It was observed that the CMR of the developed system surpassed that of the commercial ESS from a distance 100 cm onwards from the nozzle tip.
- The CMR for commercial unit radically lowered from 2.12 $mC.kg^{-1}$ to 0.561 $mC.kg^{-1}$ for the corresponding increase in the distance from the nozzle tip (50 cm to 100 cm).
- The developed system shown significantly low rate of CMR reduction (1.088 $mC.kg^{-1}$ to 0.111 $mC.kg^{-1}$) in respect of distances which in turn reflected its better charge carrying capacity than the commercial unit (2.12 $mC.kg^{-1}$ to 0.022 $mC.kg^{-1}$).

The cost effectiveness of the developed system was estimated in terms of initial cost of the equipment, quantity of chemical used, cost of cultivation and environmental contamination.

- The cost of developed system was $1/8^{th}$ of that of the commercial electrostatic (ESS-MBP90) system without compromising the performance viz. charge induction, deposition efficiency and in environmental friendly application.

REFERENCES

Alamuhanna, E. A. and Maghirang, R. G. 2010. Measuring the electrostatic charge of airborne particles. *J. Fd., Agric. & Environ.,* 8(3): 1033-1036.

Almekinders, H., Ozkan, H. E., Reichard, D. L., Carpenter, T. G. and Brazee, R. D. 1992. Spray deposition patterns of an electrostatic atomizer. *Trans. ASAE.* 36(6): 1361-1367.

Anantheswaran, R. C. and Law, S. E. 1989. Electrostatic spraying of turf grass. *VSGA, Green Section Project Rec.* pp.1-4.

Barbosa, R. N., Griffin, J. L. and Hollier, C. A. 2009. Effect of spray rate and Method of application in spray deposition. *Appl. Eng. in Agric.* American Society of Agricultural and Biological Engineers. 25(2): 181-184.

Bayat, A., Zeren, Y. and Rifat, M. V. 1994. Spray deposition with conventional and electrostatically charged spraying in citrus trees. *Agric. Mech. Asia, Afr. and Latin Am.* 25(4): 35-39.

Bode, L. E. and Bowen, H. D. 1991. Spray distribution and charge-mass ratio of electrostatically charged agricultural sprays. *Trans. ASAE.* 34(5): 1928-1934.

Bouse, L. F. 1994. Effect of nozzle type and operation on spray droplet size. *Trans. ASAE.* pp.1389-1400.

Carlton, J. B. and Bouse, L. F. 1980. Electrostatic spinner-nozzle for charging serial sprays. *Trans. ASAE.* 37(5): 1369-1374.

Carlton, J. B., Bouse, L. F. and Kirk, I. W. 1995. Electrostatic charging of aerial spray over cotton. *Trans. ASAE.* 38(6): 1641-1645.

Celen, H. I., Durgut, M. R., Gurkan, G. A. and Erdal, K. 2009. Effect of air assistance on deposition distribution of spraying by tunnel type sprayer. *Afr. J. Agric. Res.* 4(12): 1392-1397.

Derksen, R. C. and Bode, L. E. 1986. Droplet size comparison from Rotary atomizers. *Trans. ASAE.* 29(5): 1204-1207.

Fritz, B. K., Parker, C., Lopez, J. D., Hoffmann, W. C. and Schleider, P. 2009. .deposition and Droplet sizing characterization of a laboratory spray table. *Appl. Eng. in Agric.* American Society of Agricultural and Biological Engineers. 25(2): 175-180.

Gupta, C. P., Singh, G., Parameshwarkumar, M. and Ganapathy, S. 1989. Farmer driven electrostatic low-volume sprayer. *Innovative Scient. Res. U.S.-Israel CDR program, AIT, Bangkok.* pp.1-21.

Gupta, C. P., Singh, G., Muhamein, M. and Dante, E. T. 1992. Field performance of a hand-held electrostatic spinning-disc sprayer. *Trans. ASAE.* 35(6): 1753-1758.

Gupta, C. P., Alamban, R. B. and Dante, E. T. 1994. Development of knapsack electrostatic spinning disc sprayer for herbicide application in rice. *Agric. Mech. Asia, Afr. and Latin Am.* 25(4): 31-37.

Jaworek, A., Sobczyk, A. J., Krupa, A., Lackowski, M. and Czech, T. 2009. Electrostatic deposition of nano-thin films on metal substrate. *Bull. The Polish Sci.* 57(1): 63-70.

Johannama, M. R., Watkins, A. P. and Yule, A. J. 1991. Examination of electrostatically charged spray for agricultural spraying applications. *ILASS-Europe'99.* pp.1-6.

Jorg, F. and Launter, S. 2006. Electrical signals and their physiological significance in plants. *Plant, Cell and Environ.* 30(1): 249-257.

Khadir, A. I., Carpenter, T. G. and Reichard, D. L. 1994. Effects of air jets on deposition of charged spray in plant canopies. *Trans. ASAE.* 37(5): 1423-1429.

Kihm, K. D., Kim, B. H. and McFarland, A. R. 1992. Atomization, Charge and Deposition characteristics of bipolarly charged aircraft sprays. *Atomization and Sprays.* 2: 463-481.

Kirk, I. W., Hoffmann, W. C. and Carlton, J. B. 2001. Aerial electrostatic spray system performance. *Trans. ASAE.* 44(5): 1089-1092.

Krause, C. R. and Derksen, R. C. 1991. Comparison of electrostatic and cold-fog sprayers using cold-field emission scanning electron microscopy and energy dispersive X-ray microanalysis. *USDA Agric. Res. Serv., Madison-Wooster, USA.* pp.1-7.

Lake, J. R. and Merchant, J. A. 1984. Wind tunnel experiments and mathematical model of electrostatic spray deposition in Barley. *J. Agric. Eng. Res.* 30: 185-195.

Lane, M. D. and Law, S. E. 1982. Transient charge transfer in living plants undergoing electrostatic spraying. *Trans. ASAE.* 31(4): 1148-1155.

Latheef, M., Kirk, I. W., Carlton, J. B. and Hoffmann, W. C. 2008. Aerial electrostatic charged sprays for deposition and efficacy against sweet potato whitefly (*Bemisiatabaci*) on cotton. *Pest Mgmt. Sci., Wiley Interscience.* 65: 744-752.

Laryea, G. N. and No, S. Y. 2002. Spray characteristics of charge injected electrostatic pressure-swirl nozzle. *ILASS-Zaragoza, Europe.* 9(11): 1-6.

Law, S. E. 1975. Electrostatic induction instrument for tracking and charge measurement of airborne agricultural particulates. *Trans. ASAE.* pp.40-47.

Law, S. E. and Michael, D. L. 1981. Electrostatic deposition of pesticide spray onto foliar targets of varying morphology. *Trans. ASAE.* pp.1441-1445.

Law, S. E. and Cooper, S. C. 1988. Depositional characteristics of charged and uncharged droplets applied by an orchard air carrier sprayer. *Trans. ASAE.* 31(4): 984-989.

Law, S. E. and Scherm, H. 1991. Electrostatic application of a plant-disease bio-control agent for prevention of fungal infection through stigmatic surfaces of blueberry. pp.1-14.

Luciana, N. and Cramariuc, R. 2009. Contribution about the electrohydrodynamicspraying. *U.P.B. Sci. Bull., Ser.-C.* 71(3): 205-213.

Mamidi, V., Ghanashyam, C., Patel, M. K., Reddy, V. and Kapur, P. 2012. Electrostatic hand presuure swirl nozzle for small crop growers. *Int. J. Appl. Sci. & Tech., Res. Excellence.* 2(2): 164-168.

Maynagh, B., Ghobadian, B., Johannama, M. and Hashjin, T. 2009. Effect of electrostatic induction parameters on droplet charging for agricultural application. *J. Agric. Sci. & Tech.* 11(1): 249-257.

Mishra, P.K., Singh, M., Sharma, A., Sharma, K. and Singh, B. 2014. Studies on effect of electrostatic spraying in orchards. *Agric. Eng. Int., J. CIGR.* 16(3): 60-69.

Mouel, J. L., Gibert, D. and Poirier, J. P. 2010. On transient electric potential variations in standing tree and atmospheric electricity. *Comptes Rendus Geosci., Elsevier.* 342: 95-99.

Oyarace, P. and Luis, G. 2010. Electrical signals in Avocado trees – Responses to light and water availability conditions. *Plant Signaling and & Behavior, Landes Biosci.* 5(1): 34-41.

Patel, M. K., Sahoo, H. K., Nayak, M. K., Kumar, A., Ghanashyam, C. and Amod, K. 2015. Electrostatic Nozzle: New Trends in Agricultural Pesticide Spraying. *Int. J. Electr. & Electronics Eng.*, pp.6-11.

Robson, S., Mauri, M. T., Fernandes, H. C., Monteiro, P. M., Rodrigues and Cleyton, B. A. 2013. Parameters of electrostatic spraying and its influence on the application efficiency. *Rev. Ceres*, Vicosa-Brazil, 60(4): 474-479.

Sidahmed, M. M. 1996a. Theory of predicting the size and velocity of droplets from pressure nozzles. *Trans. ASAE.* 35(5): 385-391.

Sidahmed, M. M. 1996b. Theory of predicting the size and velocity of droplets from pressure nozzles. *Trans. ASAE.* 35(5): 1651-1655.

Smith, D. B., Goering, C. E., Liljeldahl, L. A., Reichard, D. L. and Gebhardt, M. R. 1977. AC charging of Agricultural sprays. *Trans. ASAE.* 34(6): 1002-1007.

Sumner, H. R., Herzog, G. A., Sumner, P. E., Bader, M. and Mullinix, B. G. 2000. Chemical application equipment for improved deposition in cotton. *J. Cott.Sci.* 4: pp.19-27.

Tong-Xian, L., Philip, A. S. and Conner, J. M. 2004. Evaluation of spray deposition on plant foliage with self-adhesive paper targets. *Subtropical Plant Sci.* 36: 39-43.

Yu, R., Zhou, H. and Zheng, J. 2011. Design and experiments on droplet charging device for high range electrostatic sprayer. *Pestcides in Modern Wld. – Pestcide Use and Mgmt.,* pp.137-148.

Walker, T. J., Dennis, R. G. and Gary, W. H. 1989. Field testing of several pesticide spray atomizers. *Trans. ASAE.* 5(3): 319-323.

Wang, L., Zhang, N., Slocombe, J. W., Thierstein, G. E. and Kuhlman, D. K. 1995. Experimental analysis of spray distribution pattern uniformity for agricultural nozzles. *Appl. Eng. in Agric.* 25(2): 50-55.

APPENDIX I

Charge carrying capacity for Model III at specific electrode placement positions

Electrode placement position	Charging Voltage Potential (kV)				
	1	**2**	**3**	**4**	**5**
CMR (mC.kg^{-1}) at 50 cm away from nozzle					
0 mm	0.111	0.311	0.533	0.667	0.777
5 mm	0.133	0.333	0.600	0.733	0.888
10 mm	0.111	0.288	0.488	0.644	0.844
15 mm	0.067	0.177	0.377	0.577	0.755
CMR (mC.kg^{-1}) at 100 cm away from nozzle					
0 mm	0.066	0.222	0.422	0.622	0.711
5 mm	0.088	0.266	0.522	0.688	0.822
10 mm	0.066	0.111	0.444	0.642	0.755
15 mm	0.060	0.100	0.377	0.555	0.644
CMR (mC.kg^{-1}) at 150 cm away from nozzle					
0 mm	0.033	0.066	0.155	0.200	0.244
5 mm	0.033	0.111	0.200	0.222	0.288
10 mm	0.022	0.044	0.066	0.133	0.200
15 mm	0.011	0.033	0.056	0.088	0.133
CMR (mC.kg^{-1}) at 200 cm away from nozzle					
0 mm	0	0	0.022	0.044	0.088

5 mm	0	0.011	0.044	0.066	0.133
10 mm	0	0	0.022	0.055	0.066
15 mm	0	0	0.011	0.444	0.060
CMR ($mC.kg^{-1}$) at 250 cm away from nozzle					
0 mm	0	0	0.022	0.044	0.066
5 mm	0	0	0.022	0.055	0.067
10 mm	0	0	0.011	0.044	0.600
15 mm	0	0	0.011	0.033	0.056

APPENDIX II

Charge carrying capacity for Model IV at specific electrode placement positions

Electrode placement position	Charging Voltage Potential (kV)				
	1	**2**	**3**	**4**	**5**
CMR (mC.kg^{-1}) at 50 cm away from nozzle					
0 mm	0.133	0.289	0.400	0.444	0.677
5 mm	0.155	0.422	0.488	0.644	0.777
10 mm	0.222	0.311	0.400	0.511	0.688
15 mm	0.133	0.177	0.333	0.355	0.588
CMR (mC.kg^{-1}) at 100 cm away from nozzle					
0 mm	0.066	0.200	0.266	0.377	0.555
5 mm	0.067	0.222	0.333	0.444	0.566
10 mm	0.066	0.155	0.220	0.288	0.466
15 mm	0.055	0.133	0.200	0.244	0.377
CMR (mC.kg^{-1}) at 150 cm away from nozzle					
0 mm	0.022	0.066	0.88	0.111	0.200
5 mm	0.033	0.067	0.113	0.177	0.266
10 mm	0.022	0.066	0.111	0.155	0.222
15 mm	0.021	0.060	0.088	0.111	0.177
CMR (mC.kg^{-1}) at 200 cm away from nozzle					
0 mm	0	0.011	0.033	0.055	0.075

5 mm	0	0.022	0.055	0.066	0.088
10 mm	0	0.011	0.022	0.055	0.066
15 mm	0	0	0.011	0.022	0.055
CMR (mC.kg^{-1}) at 250 cm away from nozzle					
0 mm	0	0	0.011	0.055	0.066
5 mm	0	0.011	0.044	0.056	0.067
10 mm	0	0.011	0.022	0.044	0.055
15 mm	0	0	0.011	0.026	0.046

APPENDIX III

Charge carrying capacity for Model V at specific electrode placement positions

Electrode placement position	**Charging Voltage Potential (kV)**				
	1	**2**	**3**	**4**	**5**
CMR (mC.kg^{-1}) at 50 cm away from nozzle					
0 mm	0.444	0.555	0.777	0.933	1.088
5 mm	0.444	0.566	0.822	0.977	1.088
10 mm	0.444	0.555	0.666	0.777	0.888
15 mm	0.422	0.511	0.533	0.711	0.822
CMR (mC.kg^{-1}) at 100 cm away from nozzle					
0 mm	0.177	0.222	0.288	0.444	0.600
5 mm	0.	0	0	0	0

	177	.266	.333	.555	.666
10 mm	0.133	0.155	0.266	0.442	0.533
15 mm	0.067	0.133	0.222	0.400	0.511
CMR (mC.kg^{-1}) at 150 cm away from nozzle					
0 mm	0.055	0.088	0.177	0.266	0.355
5 mm	0.067	0.111	0.244	0.355	0.444
10 mm	0.055	0.088	0.222	0.266	0.333
15 mm	0.044	0.067	0.155	0.222	0.311
CMR (mC.kg^{-1}) at 200 cm away from nozzle					
0 mm	0.022	0.022	0.066	0.111	0.155
5 mm	0.033	0.044	0.067	0.133	0.177
10 mm	0	0.022	0.055	0.088	0.155
15 mm	0	0.011	0.044	0.088	0.133
CMR (mC.kg^{-1}) at 250 cm away from nozzle					
0 mm	0	0	0.022	0.066	0.088
5 mm	0	0.022	0.066	0.088	0.111
10 mm	0	0.011	0.044	0.066	0.088
15 mm	0	0	0.022	0.044	0.055

APPENDIX IV

Multiple Comparison Test for EPP on CMR

(I) EPP	(J) EPP	Mean Difference (I-J)	Sig. (*p*)	Remark
At 50 cm coaxially ahead of nozzle tip				
0 mm	5 mm	-0.0118*	0.000	S
	10 mm	-0.0015	0.608	NS
	15 mm	-0.0022	0.433	NS
5 mm	0 mm	0.0118*	0.000	S
	10 mm	0.0103*	0.000	S
	15 mm	0.0095*	0.001	S
10 mm	0 mm	0.0015	0.608	NS
	5 mm	-0.0103*	0.000	S
	15 mm	-0.0008	0.786	NS
15 mm	0 mm	0.0022	0.433	NS
	5 mm	-0.0095*	0.001	S
	10 mm	0.0008	0.786	NS
At 100 cm coaxially ahead of nozzle tip				
0 mm	5 mm	-0.0118*	0.000	S
	10 mm	-0.0015	0.608	NS
	15 mm	-0.0022	0.433	NS
5 mm	0 mm	0.0118*	0.000	S
	10 mm	0.0103*	0.000	S
	15 mm	0.0095*	0.001	S
10 mm	0 mm	0.0015	0.608	NS
	5 mm	-0.0103*	0.000	S
	15 mm	-0.0008	0.786	NS
15 mm	0 mm	0.0022	0.433	NS
	5 mm	-0.0095*	0.001	S
	10 mm	0.0008	0.786	NS

At 150 cm coaxially ahead of nozzle tip				
0 mm	5 mm	-0.0118*	0.000	S
	10 mm	-0.0015	0.608	NS
	15 mm	-0.0022	0.433	NS
5 mm	0 mm	0.0118*	0.000	S
	10 mm	0.0103*	0.000	S
	15 mm	0.0095*	0.001	S
10 mm	0 mm	0.0015	0.608	NS
	5 mm	-0.0103*	0.000	S
	15 mm	-0.0008	0.786	NS
15 mm	0 mm	0.0022	0.433	NS
	5 mm	-0.0095*	0.001	S
	10 mm	0.0008	0.786	NS
At 200 cm coaxially ahead of nozzle tip				
0 mm	5 mm	-0.0118*	0.000	S
	10 mm	-0.0015	0.608	NS
	15 mm	-0.0022	0.433	NS
5 mm	0 mm	0.0118*	0.000	S
	10 mm	0.0103*	0.000	S
	15 mm	0.0095*	0.001	S
10 mm	0 mm	0.0015	0.608	NS
	5 mm	-0.0103*	0.000	S
	15 mm	-0.0008	0.786	NS
15 mm	0 mm	0.0022	0.433	NS
	5 mm	-0.0095*	0.001	S
	10 mm	0.0008	0.786	NS
At 250 cm coaxially ahead of nozzle tip				
0 mm	5 mm	-0.0118*	0.000	S
	10 mm	-0.0015	0.608	NS
	15 mm	-0.0022	0.433	NS

5 mm	0 mm	0.0118*	0.000	S
	10 mm	0.0103*	0.000	S
	15 mm	0.0095*	0.001	S
10 mm	0 mm	0.0015	0.608	NS
	5 mm	-0.0103*	0.000	S
	15 mm	-0.0008	0.786	NS
15 mm	0 mm	0.0022	0.433	NS
	5 mm	-0.0095*	0.001	S
	10 mm	0.0008	0.786	NS
*The mean difference is significant at the 0.05 level.				

DEVELOPMENT OF LOW COST ELECTROSTATIC SPRAY-CHARGING SYSTEM FOR LIQUID FORMULATIONS

By

DIPAK S. KHATAWKAR

ABSTRACT OF THE THESIS

Submitted in partial fulfilment of the requirement for the degree

Master of Technology
in
Agricultural Engineering

Faculty of Agricultural Engineering and Technology
Kerala Agricultural University

Department of Farm Power, Machinery and Energy
KELAPPAJI COLLEGE OF AGRICULTURAL ENGINEERING AND TECHNOLOGY,
TAVANUR – 679 573, MALAPPURAM DISTRICT,
KERALA
2016

ABSTRACT

The introduction of electrically charged sprays in agricultural application has become inevitable for better control on droplet transference with reduced drift and increase in application efficiency with less spray chemical requirements. In the present study was under taken to develop an electrostatic induction spray charging system as attachment to powered knapsack mist-blower. A high voltage generator was fabricated on the basis of Cockcroft-Walton voltage multiplier principle with input of 6 V DC battery to provide high voltage required at the developed charging electrode assembly (Model III, Model IV and Model V) for inducing electrostatic charge on spray droplets. As the existing (Model I) and redesigned (Model II) nozzle failed to give fine atomization, a self-atomizing hydraulic nozzle was developed for delivering the droplet spectrum required for effective electrostatic charge induction. The three working models (III, IV and V) were evaluated for charge to mass ratio ($mC.kg^{-1}$) at five electrode potentials (1 kV, 2 kV, 3 kV, 4 kV and 5 kV), four electrode placement positions (0 mm, 5 mm, 10 mm and 15 mm) and five distances (50 cm, 100cm, 150 cm, 200 cm and 250 cm) from the nozzle. Model V with electrode voltage potential at 5 kV and EPP at 5 mm shown the maximum CMR value (1.088 $mC.kg^{-1}$), followed by Model III (0.888 $mC.kg^{-1}$) and Model IV (0.777 $mC.kg^{-}1$) with same combination of variables. In contrast with commercial system (ESS-MBP90) it was observed that except at 50 cm distance from nozzle, Model V (at 4 kV and 5 kV) surpassed commercial system in CMR from 100 cm to 250 cm distance. To avoid air blast injury of plant, the nozzle has to be 100 cm to 150 cm away from the plant. The droplet spectrum of the developed system was analysed and observed that the size of droplets were 100 to 200 µm. The deposition efficiency of the developed system was on par with that commercial unit, and was within the range of 60 to 70 per cent. The developed system found to be cost effective and significantly consistent than the commercial system.

****